Inorganic Chemistry

Article

pubs.acs.org/IC

Synthesis and Reactivity of NHC-Based Rhodium Macrocycles

Rhiann E. Andrew and Adrian B. Chaplin*

Department of Chemistry, University of Warwick, Gibbet Hill Road, Coventry CV4 7AL, United Kingdom

Supporting Information

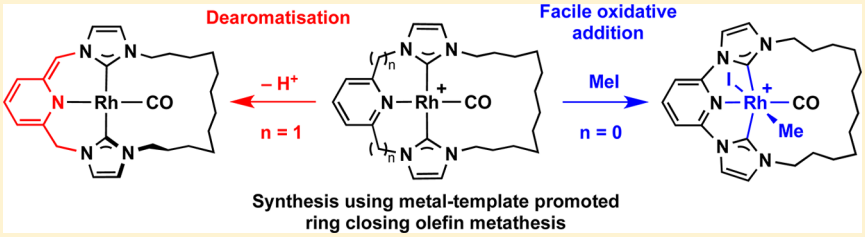

ABSTRACT: Using a general synthetic procedure employing readily accessed terminal alkene-functionalized pro-ligands and macrocyclization by ring-closing olefin metathesis, rhodium carbonyl complexes have been prepared that contain lutidine (**1a**; n = 1) and pyridine (**1b**; n = 0) derived tridentate CNC macrocycles with dodecamethylene spacers. In solution, **1a** shows temperature-invariant time-averaged C_2 symmetry by ^{1}H NMR spectroscopy (CD_2Cl_2, 500 MHz), whereas in the solid-state, two polymorphs can be obtained showing different conformations of the alkyl spacer about the metal−carbonyl bond (asymmetric and symmetric). In contrast, time-averaged motion of alkyl spacer in **1b** can be halted by cooling below 225 K (CD_2Cl_2, 500 MHz), and the complex crystallizes as a dimer with an interesting unsupported Rh···Rh bonding interaction (3.2758(6) Å). Oxidative addition reactions of **1a** and **1b**, using MeI and $PhICl_2$, have been studied in situ by ^{1}H NMR spectroscopy, although pure Rh(III) adducts can be ultimately isolated only with the pyridine-based macrocyclic ligand. The lutidine backbone of **1a** can be deprotonated by addition of $K[N(SiMe_3)_2]$, and the resulting neutral dearomatized complex (**5**) has been fully characterized in solution, by variable-temperature ^{1}H NMR spectroscopy, and in the solid state, by X-ray diffraction.

INTRODUCTION

Complexes bearing *mer*-tridentate 'pincer' ligands continue to find diverse applications in organometallic chemistry and catalysis.[1] Pincer ligands confer thermal stability and support a broad range of metal-based reactivity; reactivity that can be tuned by variation of both the axial and equatorial donors. Phosphine-based systems bearing a central aryl donor (PCP) are among the most widely studied, with iridium derivatives being notable for their high activity as alkane dehydrogenation catalysts (e.g., **A**, Chart 1).[2] Recently, lutidine-derived pincer ligands have also become prominent and can support bifunctional metal−ligand reactivity through base-induced pyridine dearomatization (e.g., leading to **B**).[3−5] Alongside the ever-growing interest in N-heterocyclic carbene (NHC) ligands, CCC and CNC pincer architectures featuring *trans*-NHC donors have been prepared and partnered with a wide variety of transition elements.[6] Palladium(II)-based CCC and CNC complexes have been shown to be catalytically active in C−C coupling reactions, and recently, inspired by work using PCP ligands, Chianese and co-workers have used analogous NHC-based variants in iridium-catalyzed alkane dehydrogenation reactions (e.g., **C**).[7,8]

Chart 1. Iridium Pincer Complexes

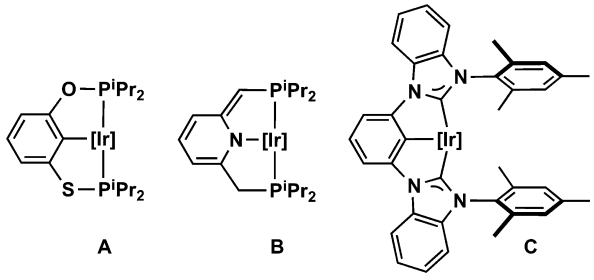

Despite facile synthetic procedures for imidazolium-based pro-ligands, the vast majority of reported CNC and CCC complexes feature NHC donors bearing simple alkyl (e.g., Me, ^{n}Bu, ^{t}Bu) and aryl (e.g., Mes, Dipp) appendages. Expanding on a limited number of prior examples,[9] we have recently begun exploring the coordination chemistry of macrocyclic ligands based on CNC pincer scaffolds. Our interest in this ligand topology is motived by the potential to (a) reinforce the thermal stability associated with pincer ligands through the macrocyclic effect, (b) exploit additional reaction control though their unique steric profile, especially through wiper-blade-like motion of the linking group, and (c) construct interlocked molecular assemblies using active-metal template strategies.[10] As part of these investigations, we have previously prepared palladium(II) derivatives of lutidine-derived CNC macrocyclic ligands containing aliphatic spacers of different length (**D**, Chart 2) and reported on how the ring size alters the

Received: October 10, 2014
Published: December 10, 2014

Chart 2. Complexes Containing CNC Pincer Ligands

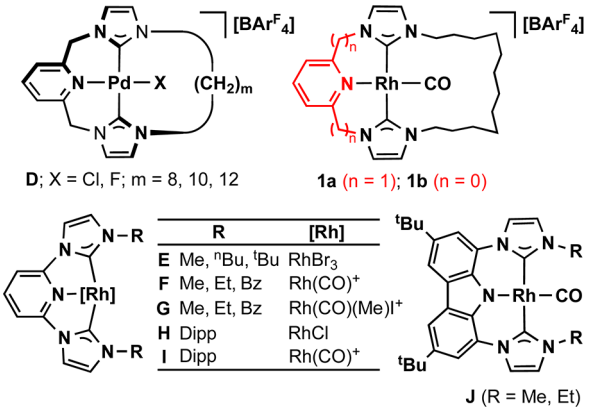

structure and dynamics of the d^8 square planar complexes.[11] Significant ground-state steric effects are induced using the shorter spacers (m = 8, 10), whereas the dodecamethylene spacer (m = 12) enabled distortion-free accommodation of ancillary ligands (X = Cl, F) within the macrocycle. In this article, we expand upon the coordination chemistry of CNC macrocycles containing the latter aliphatic chain length. In particular, we describe synthetic methodology, involving olefin metathesis, that allows the preparation of NHC-based rhodium macrocycles containing both lutidine (n = 1) and pyridine (n = 0) derived CNC pincer scaffolds with dodecamethylene spacers (**1**, Chart 2). The influence of the pincer backbone and macrocyclic topology on their dynamics and reactivity is examined.

There are surprisingly few rhodium complexes containing neutral CNC pincer ligands as precedents for **1**. Indeed, those that have been reported are limited to a narrow range of pyridine-bridged systems (**E**–**I**, Chart 2).[12−14] Potentially, tridentate bis(imidazolium)pyridine and bis(imidazolium)-lutidine pro-ligands have also been observed to bridge two metal rhodium centers instead when using [Rh(COD)Cl]$_2$ (COD = cyclooctadiene) as the metal precursor.[12b,15] To avoid these bimetallic products, successful chelation procedures are characterized by relatively forcing reaction conditions (e.g., reflux in aerated acetonitrile, **E**)[12] or use of rhodium precursors with more readily displaced ligands: [Rh(CO)$_2$(OAc)]$_2$ (**F**)[13] and [Rh(alkene)$_2$Cl]$_2$ (alkene = cylcooctene, ethylene; **H**).[14] Closely related anionic carbazole-based rhodium CNC complexes (**J** in Chart 2) have been prepared by Kunz and co-workers and shown to undergo facile oxidative addition reactions with alkyl, allyl, and benzyl halides.[16]

RESULTS AND DISCUSSION

Synthesis. Using our previously reported Ag$_2$O-based transmetalation strategy in combination with [Rh(CO)$_2$Cl]$_2$ and preformed macrocyclic pro-ligand **L1a**,[11] rhodium complex **1a** was obtained in a straightforward manner in good isolated yield (52%) following purification on silica and recrystallization (route 1, Scheme 1). This procedure results in the incorporation of the weakly coordinating [BAr$^F_4$]$^-$ counter-anion (Ar^F = 3,5-C$_6$H$_3$(CF$_3$)$_2$), which helps to confer solubility in a range of organic solvents including diethyl ether, benzene, and dichloromethane. Seeking to similarly prepare **1b**, we first attempted to prepare pyridine-bridged **L1b**. Although we did not exhaustively investigate all potential macrocyclization reactions, we found that direct adaption of routine literature protocols for noncyclic CNC pro-ligands,[17] involving alkylation of 2,6-bis(imidazolyl)pyridine with 1,12-dibromododecane or alkylation of 1,12-bis(imidazolyl)dodecane with 2,6-dibromo-pyridine in refluxing dioxane, gave unsatisfactory results. Consequently, to avoid the need for preformed macrocyclic pro-ligands **L1**, a metal-template-based procedure employing more accessible terminal alkene-functionalized pro-ligands **L2** was developed (route 2, Scheme 1). Macrocyclization can be achieved using sequential olefin metathesis/hydrogenation steps following coordination of the pro-ligand. Methodology of this nature is well-documented in the literature,[18] with work by Gladysz particularly noteworthy for its use of rhodium(I)-based templates.[19]

The terminal alkene functionalized pro-ligands (**L2**) were readily prepared and corresponding rhodium carbonyl adducts **2** generated using analogous reaction conditions to those used for **1a**. Purification on silica afforded **2a** (58%) and **2b** (83%) with good isolated yields. Macrocyclic derivatives **1** were then obtained from **2** by sequential olefin metathesis (Grubbs I) and hydrogenation. Under the same reaction conditions, analysis by ESI-MS revealed that the cyclization of **2b** (100% conversion within 1 h) proceeded more rapidly than that of **2a** (ca. 69% conversion after 1 h). In both systems, complete and selective macrocyclization is observed; however, the latter system

Scheme 1. Synthetic Procedures for the Preparation of 1 (a; n = 1; b, n = 0)[a]

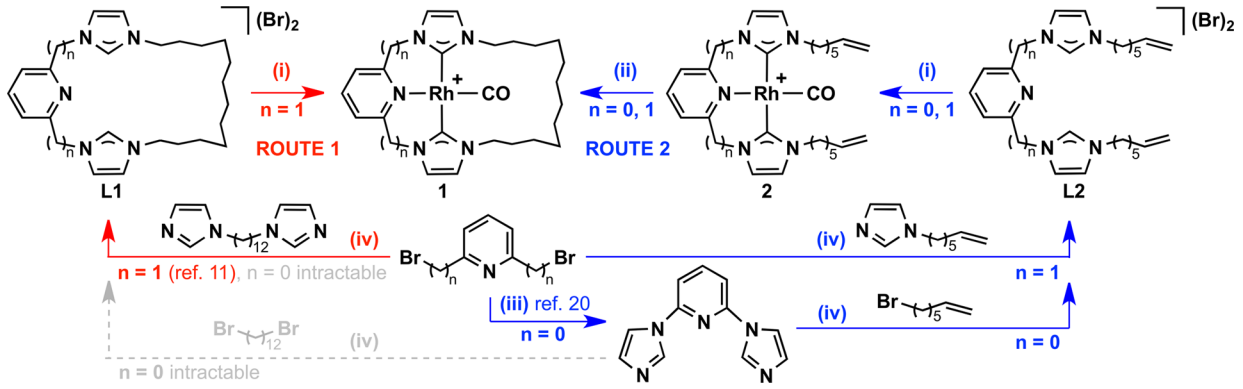

[a][BAr$^F_4$]$^-$ anions omitted for clarity. Reagents and conditions: (i) Ag$_2$O and Na[BAr$^F_4$] then [Rh(CO)$_2$Cl]$_2$ (CH$_2$Cl$_2$, RT); (ii) [**2**] ~ 1 mmol L^{-1}; Grubbs I (CH$_2$Cl$_2$, RT), followed by hydrogenation using [Ir(COD)(py)(PCy$_3$)][BAr$^F_4$] (10 mol %, 1 atm H$_2$, CH$_2$Cl$_2$, RT; n = 0) or Pd/C (20 mol %, 4 atm H$_2$, CH$_2$Cl$_2$, RT; n = 1); (iii) imidazole, K$_2$CO$_3$, DMF, 150 °C (ref 20); (iv) 1,4-dioxane, reflux.

dx.doi.org/10.1021/ic5024828 | Inorg. Chem. 2015, 54, 312−322

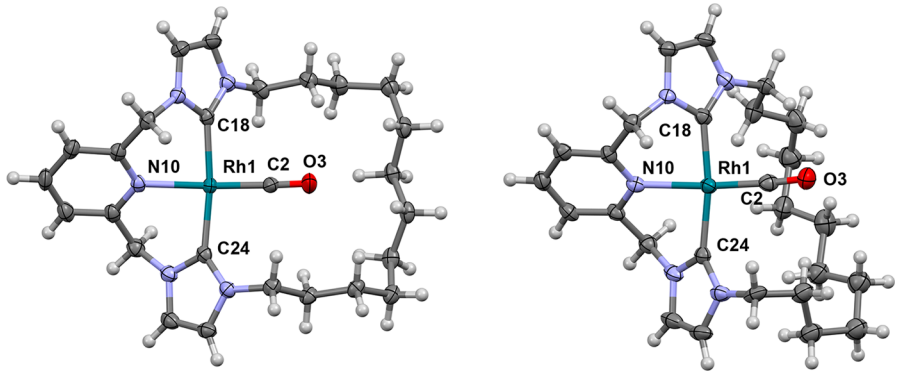

Figure 1. Solid-state structures of **1a**/**1a***. Thermal ellipsoids are drawn at the 50% (left, symmetrical; **1a**) and 30% (right, asymmetrical; **1a***) probability levels; minor disordered components and anions are omitted for clarity. Selected bond lengths (Å) and angles (deg): (**1a**) Rh1−C2, 1.804(3); Rh1−N10, 2.134(2); Rh1−C18, 2.036(3); Rh1−C24, 2.042(3); C2−O3, 1.148(4); N10−Rh1−C2, 175.16(13); C18−Rh1−C24, 172.77(12); C11−C16−N17, 112.1(3). (**1a***) Rh1−C2, 1.796(9); Rh1−N10, 2.150(7); Rh1−C18, 2.020(7); Rh1−C24, 2.038(7); C2−O3, 1.153(11); N10−Rh1−C2, 175.0(3); C18−Rh1−C24, 169.9(3); C11−C16−N17, 110.8(6).

Table 1. Solution and Solid-State Characterization Metrics for 1−5[a]

	ancillary ligands	ν(CO)/cm^{-1}	$\delta_{\underline{C}O}$ (J_{RhC}/Hz)	$\delta_{N\underline{C}N}$ (J_{RhC}/Hz)	r(Rh$\underline{C}$O)/Å	r(RhN)/Å	r(RhC_{CNC})/Å	$\angle$(C_{NCN}RhC_{NCN})/°
1a	CO	1979 1972[b]	194.0(80)	181.8(42)	1.804(3); 1.796(9)[c]	2.134(2); 2.150(7)[c]	2.036(3), 2.042(3); 2.020(7), 2.038(7)[c]	172.77(12); 169.9(3)[c]
2a	CO	1978	193.9(79)	182.2(41)				
3a	(CO)(Me)I	2067	189.4(64)	165.1(34)				
4a	$(CO)Cl_2$	2110	180.7(57)	160.1(30)				
5[b]	CO	1929	197.4(73)	185.5(43), 174.2 (44)	1.799(3)	2.113(2)	2.048(3), 2.045(3)	170.45(10)
1b	CO	1986 1977[d]	196.8(78)	186.5(48)	1.836(4)	2.027(3)	2.029(4), 2.028(4)	155.18(15)
2b	CO	1990 1980[d]	[e]	186.6(48)				
3b	(CO)(Me)I	2070 2066[d]	189.8(61)	180.2(37)	1.869(4)	2.005(3)	2.041(3), 2.028(3)	156.47(15)
4b	$(CO)Cl_2$	2111	181.6(57)	173.9(33)	1.945(3)	1.997(3)	2.043(3), 2.049(3)	156.47(12)

[a]IR spectra were recorded in CH_2Cl_2; NMR spectra were recorded in CD_2Cl_2. [b]Measured in C_6H_6 (IR) or C_6D_6 (NMR). [c]Asymmetrical polymorph (**1a***). [d]Measured in MeCN. [e]Resonance not observed.

required an additional portion of catalyst for full cyclization. This difference in reactivity is entirely consistent with the more favorable ligand substituent geometry of the planar, pyridine-based **L2b** ligand. Hydrogenation of the resulting internal alkene groups using Pd/C (4 atm H_2) was effective for both systems, although, under these conditions, **1b** was found to be unstable.[21] Consequently, preparation of **1b** was instead carried out using $[Ir(COD)(py)(PCy_3)][BAr^F{}_4]$ as the catalyst,[22] enabling rapid and selective hydrogenation of the internal alkene group (10 mol % catalyst, 1 atm H_2). Ultimately, despite these subtle differences in conditions, high purity samples of **1** were readily obtained from **2** in high isolated yields of 78% (**1a**) and 68% (**1b**) over two steps. With 2,6-bis(bromomethyl)-pyridine as a common precursor, the effectiveness of each synthetic procedure can be evaluated for **1a**. Although the reactions were not fully optimized, route 2 noticeably gave a much greater overall yield (43% over four steps) in comparison to that of route 1 (20% over two steps), principally due to the low-yielding preparation of **L1a** (39%) compared to **L2a** (94%).[11]

Characterization. In CD_2Cl_2 solution, **1a** is C_2 symmetric, with diagnostic diastereotopic resonances for the methylene bridge protons (py$C\underline{H}_2$) observed at δ 5.45 and 5.03 ($^2J_{HH}$ = 14.7 Hz) in the ^{1}H NMR spectrum (298 K, 500 MHz), a geometry characteristic of lutidine-derived pincer ligands.[6,7,23] In line with preceding work using palladium,[11] this time-averaged symmetry is fully retained on cooling to 185 K (see Figure S10). High symmetry is also adopted in a solid-state X-ray structure of **1a** obtained using single crystals grown from diethyl ether−hexane under an inert atmosphere (Figure 1, left). The ancillary carbonyl ligand notably binds with a Rh1−C2 bond distance of 1.804(3) Å and is well-accommodated within the cavity of the macrocycle; the alkyl spacer is only slightly askew. We have also obtained a much more asymmetric solid-state structure when crystallization was carried out under nonroutine conditions using a different solvent combination (CH_2Cl_2−pentane, 1 atm CO). In this polymorph (**1a***), the alkyl spacer is instead completely twisted to one side of the molecule, resulting in unmistakable C_1 symmetry (Figure 1, right). Despite the large difference in alkyl spacer conformation, the structural metrics indicate that the geometries about the rhodium center are very similar: both show little distortion from square planar geometry with ideal sum of angles (360.1(5)°, **1a**; 360.2(12)°, **1a***) and essentially linear N10−Rh1−C2 bond angles (175.16(13)°, **1a**; 175.0(3)°, **1a***). Other key parameters are summarized in Table 1. We suggest the formation of the asymmetrical polymorph results from reversible carbon monoxide coordination during crystallization, although we cannot rule out crystal-packing effects.[24] Notwithstanding the origin of the polymorphism, the solid-

dx.doi.org/10.1021/ic5024828 | Inorg. Chem. 2015, 54, 312−322

state structures illustrate the full range of conformational flexibility accessible in the macrocyclic system. Ultimately, in solution, the variable-temperature NMR data clearly show that the carbonyl ligand does little to impede dynamic movement of the dodecamethylene spacer. A conclusion that is also supported by the similarity of spectroscopic data gathered for **1a** and noncyclic **2a** (Table 1). Notably, no macrocycle effect is apparent on comparison of the carbenic and carbonyl ^{13}C resonances (ca. δ 182 ($^1J_{RhC}$ ca. 40 Hz) and ca. δ 194 ($^1J_{RhC}$ ca. 80 Hz), respectively) and ν(CO) bands (**1a**, 1979 cm^{-1}; **2a**, 1978 cm^{-1} in CH_2Cl_2). Furthermore, despite different donor groups, data associated with the coordinated carbonyl ligand in **1a** is comparable with that found for phosphine pincer complex $[Rh(PNP^{tBu})(CO)]^+$ (PNP^{tBu} = 2,6-bis(di-*tert*-butylphosphinomethyl)pyridine), where the coordinated carbonyl ligand is characterized by δ_{13C} 196 ($^1J_{RhC}$ = 70 Hz) and ν(CO) 1982 cm^{-1} in solution and a Rh−C distance of 1.818(5) Å in the solid state.[25]

Counteracting Coulombic repulsion, **1b** interestingly crystallizes as a dimer with an unsupported Rh···Rh interaction (3.2758(6) Å) and the alkyl chain angled to one side (Figure 2). Metal−metal interactions of this nature have been

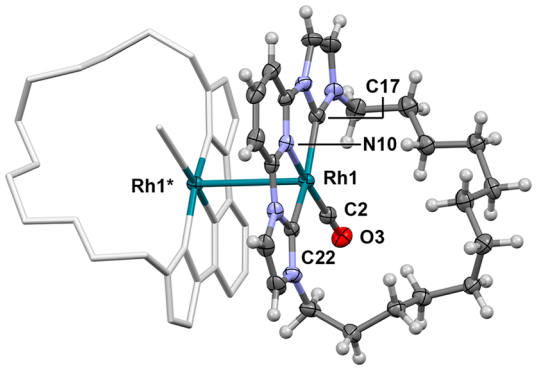

Figure 2. Solid-state structure of **1b**. Thermal ellipsoids are drawn at the 30% probability level; minor disordered components and anions are omitted for clarity; symmetry operation $-x, -y + 1, -z + 1$ was used to generate the stared atom. Selected bond lengths (Å) and angles (deg): Rh1···Rh1*, 3.2758(6); Rh1−C2, 1.836(4); Rh1−N10, 2.027(3); Rh1−C17, 2.029(4); Rh1−C22, 2.028(4); C2−O3, 1.154(5); N10−Rh1−C2, 176.08(15); C17−Rh1−C22, 155.18(15).

documented for a variety of planar d^8 transition metal compounds and are attributed to overlap of d_{z2} and p_z orbitals on the adjacent metal centers.[26−29] For comparison, in both polymorphs of nonplanar **1a**, the Rh···Rh distances are >6.0 Å. The solid-state dimer of **1b** bears striking resemblance to that formed by macrocyclic $[Rh(SNS)(CO)]^+$ (SNS = 5,8,11-trioxa-2,14-dithia[15]-(2,6)-pyridinophane), which is characterized by a Rh···Rh distance of 3.3320(6) Å and similar anti orientation of the monomers about the metal−metal vector.[28] Similar metal−metal distances are also observed in related cationic rhodium(I) isocyanide dimers (3.19−3.29 Å),[29] which have been estimated to have a bond energy of up to 18 kcal·mol^{-1}.[30] In solution, the metal−metal interaction observed for **1b** in the solid state is not retained, with concentration-invariant UV−vis absorption spectra (deep violet in CH_2Cl_2 solution) and observation of C_{2v} symmetry by NMR spectroscopy (298 K, 500 MHz). The high symmetry observed by NMR spectroscopy infers dynamic movement of the alkyl spacer across both sides of the molecule on the NMR time scale and is halted only by cooling below 225 K, where decoalescence of the N-CH_2CH_2 resonances can be noted (see Figure S13). The slow exchange limit cannot, however, be reached even on cooling to 185 K. ESI-MS revealed a parent ion signal at 508.1570 m/z (calc. 508.1578) with an integral-spaced isotope distribution, further supporting monomeric formulation of **1b** in solution. As seen with the lutidine-based ligands, spectroscopic data associated with the coordination of **L1b** and noncyclic **L2b** are remarkably similar (Table 1). Likewise, reasonably good agreement is seen between **1b**/**2b** and **F**, based on the limited data available for the latter (ν(CO) 1977/1980 vs ca. 1982 cm^{-1} in MeCN).[13] In terms of the ability to form dimers in the solid state, with no crystal structures at hand for **2b** and **F** (and to a lesser extent bulky **I**), it remains to be seen if this is a general feature of the chemistry of pyridine-based NHC pincers.

Oxidative Addition Reactions. As a means to assess differences in reactivity, we have studied oxidative addition reactions of **1** with MeI and $PhICl_2$ in CD_2Cl_2 solution by NMR spectroscopy (Scheme 2). Pyridine-based rhodium macrocyle **1b** reacted rapidly and quantitatively with MeI (3 equiv) to afford yellow Rh(III) derivative **3b** within 3 h at 293 K. Under the same conditions, however, no significant reaction was apparent for **1a**, which instead required 50 equiv MeI to promote oxidative addition (95% conversion to **3a** after 3 h). Scaling up the reaction, Rh(III) adduct **3b** was isolated in 75% yield. The structure of **3b** was firmly established by X-ray diffraction (Figure 3) and fully corroborated in solution by ^1H NMR, ^{13}C NMR, and IR spectroscopy, in addition to ESI-MS and elemental analysis. An integral 3H doublet at δ 0.59 ($^2J_{RhH}$ = 2.1 Hz) in the ^1H NMR spectrum and low-frequency ^{13}C doublet at δ −2.1 ($^1J_{RhC}$ = 18 Hz) are ascribed to the methyl ligand, which binds with a Rh1−C4 distance of 2.297(3) Å in the solid state. Moreover, the increase in formal oxidation state leads to reduced $^1J_{RhC}$ coupling constants for the NHC and carbonyl ligands (Table 1) and a significantly shifted ν(CO) band (2070 cm^{-1}, cf. 1986 cm^{-1}). Loss of symmetry as a consequence of MeI addition to **1b** is apparent both from the solid-state structure, the alkyl spacer of the macrocycle is notably skewed to one side of the complex, and NMR spectroscopy (C_s, 200−298 K, 500 MHz; Figure S18). In

Scheme 2. Reactions of 1 with MeI and $PhICl_2$[a]

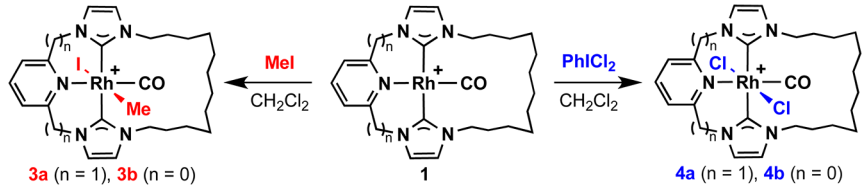

[a] $[BAr^F_4]^-$ anions omitted for clarity.

dx.doi.org/10.1021/ic5024828 | Inorg. Chem. 2015, 54, 312−322

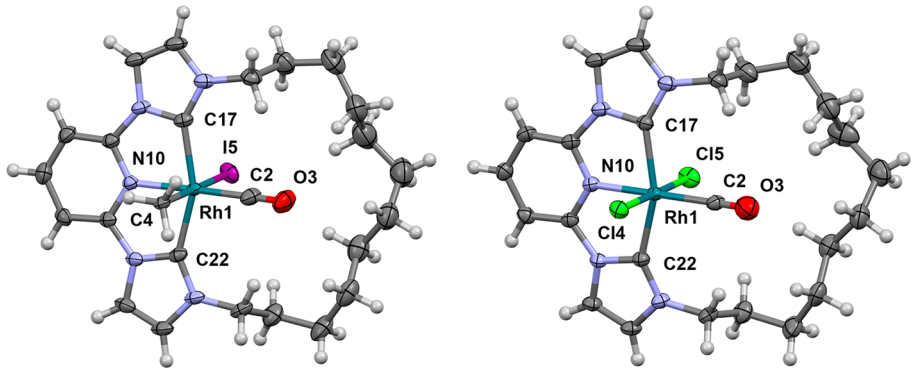

Figure 3. Solid-state structures of **3b** and **4b**. Thermal ellipsoids are drawn at the 50% probability level; minor disordered components, solvent molecule, and anions are omitted for clarity. Selected bond lengths (Å) and angles (deg): (**3b**) Rh1−C2, 1.869(4); Rh1−C4, 2.297(3); Rh1−I5, 2.7539(4); Rh1−N10, 2.005(3); Rh1−C17, 2.041(3); Rh1−C22, 2.028(3); C2−O3, 1.122(5); N10−Rh1−C2, 175.42(15); C4−Rh1−I5, 178.42(9); C17−Rh1−C22, 156.47(15); (**4b**) Rh1−C2, 1.945(3); Rh1−Cl4, 2.3514(8); Rh1−Cl5, 2.3150(8); Rh1−N10, 1.997(3); Rh1−C17, 2.043(3); Rh1−C22, 2.049(3); C2−O3, 1.046(4); N10−Rh1−C2, 178.19(11); Cl4−Rh1−Cl5, 179.49(3); C17−Rh1−C22, 156.47(12).

contrast to **3b**, our attempts to isolate pure **3a** were frustrated by the apparent instability of this species in the absence of excess MeI, and samples of high purity could not be obtained; alongside reformation of **1a** by reductive elimination of MeI, a poorly characterized C_1 symmetric species was observed by ^{1}H NMR spectroscopy. Complex **3a** was therefore characterized in situ, in the presence of excess MeI. The formation of a single oxidative addition product is confirmed by a combination of ^{1}H ($\delta_{\underline{C}H_3}$ 1.2, $^2J_{RhH}$ = 1.8 Hz) and ^{13}C ($\delta_{\underline{C}H_3}$ −1.2, $^2J_{RhH}$ = 20 Hz) NMR spectroscopy, IR spectroscopy (ν(CO) = 2067 cm^{-1}), and ESI-MS ([M]$^+$ = 678.1169 (calcd. 678.1171) m/z). We are unable to unambiguously assign the geometry of this product, but, through comparison to the spectroscopic data of **3b**, the geometry of related literature precedents,[16] and noting the C_2 symmetry observed for **4a** (vide infra), we suggest that the iodide and methyl ligands adopt a trans arrangement, as is seen for **3b**. Significant dynamic behavior of **3a** in solution is apparent by broad methylene resonances in the ^{1}H NMR spectrum at 298 K (500 MHz). Complete decoalescence is observed on cooling below 280 K, and the exchange is frozen out at 250 K, revealing C_1 geometry (see Figure S16). This dynamic behavior clearly indicates that, irrespective of the geometry of the ancillary ligands, the alkyl chain of the lutidine-based pincer ligand in **3a** is highly fluxional in solution.

Haynes and co-workers have previously studied the reaction kinetics of the closely related oxidative addition of MeI to **F** in acetonitrile, resulting in two isomeric Rh(III) species (**G**).[13] These reactions were shown to be second-order and to proceed with large negative entropies of activation, consistent with a nucleophilic oxidative addition reaction mechanism. Given the structural similarity with **F** and extensive precedents in other d^8 systems, epitomized by Vaska's complex [Ir(CO)Cl(PPh$_3$)$_2$],[31] this reaction mechanism also seems to be probable for the formation of **3** from **1**. In the absence of solid-state structures, Haynes and co-workers were unable to assign the geometry of the two isomers of **G**. By comparison of IR spectroscopic data for **3b** (ν(CO) = 2066 cm^{-1} in MeCN), the major isomers of these products are readily assigned to species with the same stereoisomerism (ν(CO) ca. 2072 cm^{-1}). The high selectively observed in the reaction of **1b** with MeI, in comparison to the nonmacrocyclic systems **F**, is interesting and hints at a non-negligible steric role of the alkyl spacer during the reaction. Subtle electronic factors cannot be ignored, however, and notably selective trans-addition of alkyl halides is observed in the reaction of related, albeit neutral, **J**.[16]

Using the oxidant PhICl$_2$,[32] a trend begins to emerge in the reactivity characteristics of the two macrocyclic NHC systems. Although Rh(III) dichloride complexes **4** readily form on reaction of 1.1 equiv of the oxidant with **1** (within 1 h), the lutidine-based derivative **4a** is unstable and appears to undergo a ligand redistribution reaction on attempted isolation, ultimately leading to intractable mixtures. Complex **4b** is, in contrast, stable and readily amenable to isolation (67% following crystallization, Figure 3). In addition to the solid-state structure of **4b**, the structures of the Rh(III) dichlorides have been fully interrogated in solution by NMR and IR spectroscopy, in addition to ESI-MS data; data for **4a** obtained in situ. Intact parent ion signals are observed in the ESI-MS spectra of both compounds: **4a**, 606.1271 (calcd. 606.1268) m/z; **4b**, 578.0958 (calc. 578.0955) m/z. The adoption of a trans-configuration for the chloride ligands is apparent from high symmetry in the ^{1}H NMR spectra of **4a** (C_2) and **4b** (C_{2v}) at 298 K (500 MHz). As for the parent compounds **1**, this high symmetry is retained only for the lutidine-based **4a** on cooling to 200 K (see Figure S21); the ^{1}H NMR spectrum of **4b** at this temperature shows C_s symmetry (see Figure S23), consistent with the skewing of the alkyl spacer to one side seen in the X-ray structure (Figure 3). As for the methyl iodide derivatives, the increase in formal state is accompanied by reduced $^1J_{RhC}$ coupling constants for the NHC and carbonyl ligands (Table 1) and a significantly shifted ν(CO) band (**4a**, 2110, cf. 1979 cm^{-1}; **4b**, 2111, cf. 1986 cm^{-1}). The latter changes in the carbonyl stretching frequencies on oxidation are noticeably more pronounced in comparison to those seen during the formation of **3**.

The oxidative addition reactions clearly indicate an increase in reactivity (MeI) and product stability (MeI and PhICl$_2$) for the pyridine-based **1b** in comparison to the lutidine-based **1a**. Electronic differences between the two complexes are evident from the carbonyl stretching frequencies in CH$_2$Cl$_2$ (**1a**, 1979 cm^{-1}; **1b**, 1986 cm^{-1}), although the values do not tally with the observed trend in reactivity; the lower value observed for **1a** would conventionally suggest a more electron-rich metal center and a greater disposition toward oxidative addition.[31] Curiously, despite the differences between the two pincer architectures found for **1**, the carbonyl bands for the corresponding Rh(III) derivatives are, however, remarkably

dx.doi.org/10.1021/ic5024828 | Inorg. Chem. 2015, 54, 312−322

Scheme 3. Formation of 5 and Closely Related Literature Precedents[a]

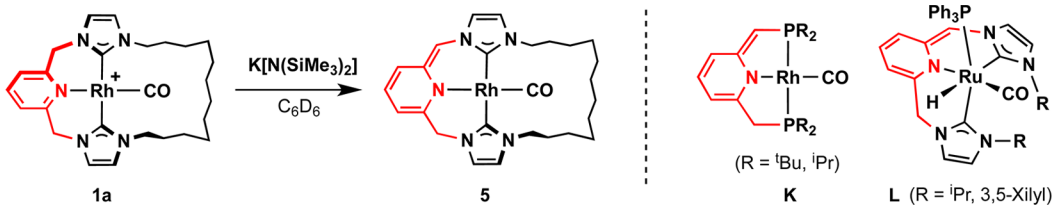

[a] $[BAr^F_4]^-$ anion omitted for clarity.

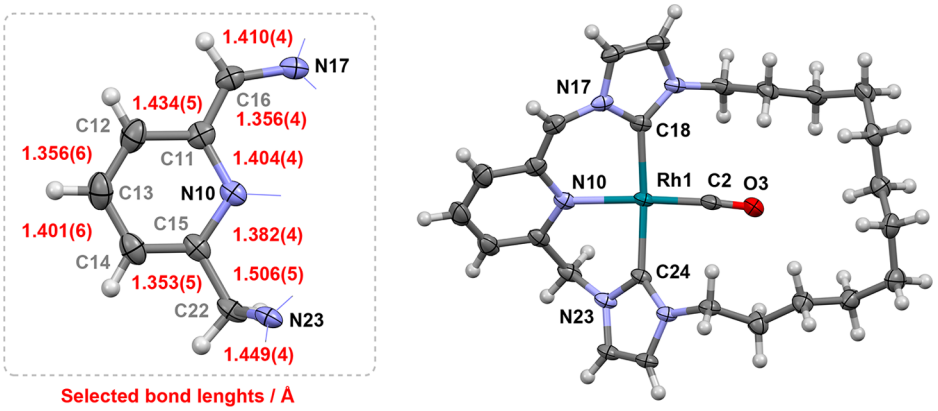

Figure 4. Solid-state structure of **5**. Thermal ellipsoids are drawn at the 30% probability level; minor disordered components and solvent omitted for clarity. Additional bond lengths (Å) and angles (deg): Rh1−C2, 1.799(3); Rh1−N10, 2.113(2); Rh1−C18, 2.048(3); Rh1−C24, 2.045(3); C2−O3, 1.149(4); N10−Rh1−C2, 172.88(11); C18−Rh1−C24, 170.45(10); C11−C16−N17, 126.7(3); C15−C22−N23, 111.3(2).

similar (**3a**, 2067 cm^{-1}; **3b**, 2070 cm^{-1}; **4a**, 2110 cm^{-1}; **4b**, 2111 cm^{-1}). Studying phosphine-based PNP rhodium systems, Milstein and co-workers have recently reported similar subtleties in the reactions of $[Rh(PNP^R)(Me)I]^+$ (R = ^{t}Bu, ^{i}Pr) with carbon monoxide.[33] Rapid reductive elimination of MeI was observed in the PNP^{t}Bu-ligated system, whereas, using the less bulky PNP^{iPr} complex, the Rh(III) adduct $[Rh(PNP^{iPr})(Me)I(CO)]^+$ could be isolated (although elimination of MeI occurs in the absence of a CO atmosphere). This reactivity strongly suggests that steric effects can play a key role in the relative stability of Rh(I) and Rh(III) fragments supported by tridentate ligands. Given the large changes in NHC-substituent geometry that result from the two central donor groups, evidenced by the highly dynamic movement of the alkyl spacer in the lutidine-based macrocyclic systems, the origin of the differences in reactivity observed between **1a** and **1b** may be predominately steric in origin. In the absence of detailed calculations, however, the precise delineation of underlying steric or electronic effects remains to be determined.

Dearomatization of 1a. In view of the low apparent stability of Rh(III) complexes of **L1a** and the increasing use of pincers as bifunctional ligands (vide supra), we sought to explore additional base-induced reactivity of **1a**. With rhodium PNP pincers **K** and ruthenium CNC pincers **L** as closely related precedents,[3,5b] the reaction of **1a** with $K[N(SiMe_3)_2]$ (1.1 equiv) in C_6D_6 at 293 K was investigated (Scheme 3). A rapid reaction was evident by an immediate change in color from yellow to deep red on mixing. Analysis by in situ ^{1}H NMR spectroscopy (298 K, 500 MHz) indicated the quantitative consumption of **1a** and formation of pyridine dearomatized **5**. The formation of **5** is associated with very notable loss in symmetry (C_1) in comparison to **1a** (C_2) and the observation of $HN(SiMe_3)_2$ (δ_{CH3} = 0.10, δ_{NH} = −0.07) in the ^{1}H and ^{13}C NMR spectra. Broadened resonances are observed for the methylene protons at 298 K (500 MHz), which sharpen on cooling to 280 K (see Figure S26). At this temperature, the vinylic proton is identified by a ^{1}H resonance at δ 5.81, alongside diastereotopic py$C\underline{H}_2$ resonances (δ 3.72, 4.58; $^2J_{HH}$ = 13 Hz) and two sets of similarly diastereotopic N-$C\underline{H}_2$ resonances. Heating the sample to 350 K results in coalescence of the methylene signals and time-averaged C_s symmetry, resulting from atropisomerization of the pincer backbone and coupled dynamics of the dodecamethylene spacer. The imidazolylidene (4 × 1H) and pyridine (3 × 1H) resonances remain sharp across the full temperature range measured (280−350 K). Complex **5** is highly reactive and best prepared and characterized in situ. Small quantities of **5** can be isolated from benzene by decantation (to remove precipitated $K[BAr^F_4]$) and layering with rigorously dried pentane (52% yield). Using this method, we have obtained single crystalline samples suitable for X-ray diffraction analysis; the resulting solid-state structure is depicted in Figure 4. Crystallographically characterized examples of group 9 dearomatized pincer complexes are scarce.[34,35] In comparison to precursor **1a**, the presence of an sp^2 carbon in the pincer backbone of **5** is readily apparent by a marked increase in the C11−C16−N17 angle (from 112.1(3)/110.8(6)° to 126.7(3)°) and contraction of the C11−C16 bond (from 1.506(5)/1.502(10) Å to 1.356(4) Å; ca. 0.15 Å). A similar, but less pronounced, bond length change was also observed on dearomatization of $[Rh(SNN)(CO)]^+$ (**M**; SNN = 2-(diethylaminomethyl)-6-(*tert*-butylsulfinylmethyl)pyridine; from 1.502(4) to 1.391(5) Å; ca. 0.11 Å).[34] Dearomatization of the CNC pincer backbone is readily apparent by bond length alternation in the pyridine ring, which is illustrated in the inset of Figure 4. The resulting amido group is associated with a slightly shortened Rh1−N10 bond (2.113(2) Å, cf. 2.134(2)/

dx.doi.org/10.1021/ic5024828 | Inorg. Chem. 2015, 54, 312−322

2.150(7) Å for **1a**) but, more noticeably, a low-frequency carbonyl band in the IR spectrum measured in C_6H_6 (1929 cm^{-1}, cf. 1972 cm^{-1} for **1a**).

SUMMARY

Building upon our previous work with palladium,[11] in this article, we have described the preparation and reactivity of rhodium complexes containing macrocyclic CNC pincer ligands. In particular, we have developed a general synthetic procedure employing readily accessed terminal alkene functionalized pro-ligands that entails sequential Ag_2O-based transmetalation, ring-closing olefin metathesis, and hydrogenation. This general procedure overcomes difficulties relating to the preparation of preformed macrocyclic pro-ligands and enabled access to both lutidine ($[Rh(C\text{^}N\text{^}C\text{-}(CH_2)_{12})(CO)]^+$, **1a**) and pyridine ($[Rh(CNC\text{-}(CH_2)_{12})(CO)]^+$, **1b**) based rhodium macrocycles in high purity and with good isolated yields. Indeed, in the case of the lutidine-based system, where a preformed macrocyclic pro-ligand can be prepared, the general procedure is twice as high yielding overall, despite double the number of steps. Altering the geometry of the pincer backbone results in marked differences in spectroscopic characteristics, overall structural dynamics, and chemical reactivity. The lutidine-based CNC systems are characterized by increased fluxional motion of the macrocycles' dodecamethylene spacer in comparison to the pyridine-based analogues. In solution, **1a** shows temperature-invariant time-averaged C_2 symmetry by ^1H NMR spectroscopy (CD_2Cl_2, 500 MHz), whereas in the solid state, two polymorphs can be obtained showing different conformations of the alkyl spacer about the metal−carbonyl bond (asymmetric and symmetric). In contrast, time-averaged motion of alkyl spacer in **1b** can be halted by cooling below 225 K (CD_2Cl_2, 500 MHz), and the complex crystallizes as a dimer with an interesting unsupported Rh···Rh bonding interaction (3.2758(6) Å). These structural variations also appear to be manifested in the reactivity of the complexes, with reaction of MeI and $PhICl_2$ leading to stable isolable Rh(III) products for **1b** only. Although the corresponding Rh(III) adducts resulting from **1a** are ultimately unstable, the backbone of the pincer can be dearomatized by addition of $K[N(SiMe_3)_2]$, accessing potential bifunctional reactivity not possible with **1b**. The resulting neutral dearomatized complex ($[Rh(C\text{^}N\text{^}C^*\text{-}(CH_2)_{12})(CO)]$, **5**) has been fully characterized in solution, by variable-temperature ^1H NMR spectroscopy, and in the solid state, by X-ray diffraction. Further investigation of the coordination and organometallic chemistry of macrocyclic CNC and CCC pincer ligands, including **1**, is ongoing in our laboratory.

EXPERIMENTAL SECTION

General Experimental Methods. Manipulations were performed under an inert atmosphere using Schlenk (dinitrogen unless otherwise stated) and glovebox (argon) techniques unless otherwise stated. Glassware was oven-dried at 130 °C overnight and flamed under vacuum prior to use. Anhydrous solvents (<0.005% H_2O) were purchased from Acros Organics or Sigma-Aldrich and used as supplied: DMF, MeCN, CH_2Cl_2, THF, 1,4-dioxane, hexane, pentane, and Et_2O. CD_2Cl_2 was dried over CaH_2, vacuum distilled, and stored under argon. C_6D_6 was dried over sodium, vacuum distilled, and stored under argon. $Na[BAr^F{}_4]$,[36] $[Rh(CO)_2Cl]_2$,[37] **L1a**,[11] 2,6-bis(imidazolyl)pyridine,[20] $PhICl_2$,[32] and $[Ir(COD)(py)(PCy_3)][BAr^F{}_4]$[22] were synthesized using literature procedures. All other solvents and reagents are commercial products and were used as received. NMR spectra were recorded on Bruker DPX-300, DPX-400, AV-400, AV-500, and AVIII-600 spectrometers at 298 K unless otherwise stated. Chemical shifts are quoted in ppm, and coupling constants, in Hz. IR spectra were recorded on a PerkinElmer Spectrum One FT-IR spectrometer. UV−vis absorption spectra were recorded on Agilent Cary 60 spectrometer. High-resolution ESI-MS were recorded on a Bruker MaXis spectrometer. Microanalyses were performed at the London Metropolitan University by Stephen Boyer.

Synthesis of New Compounds. *7-Imidazole-1-heptene.* NaH (60 wt % suspension in mineral oil, 0.32 g, 8.03 mmol) was added portionwise to a stirred solution of imidazole (0.50 g, 7.34 mmol) in 50 mL THF at 0 °C, over 5 min. 7-Bromo-1-heptene (1.18 mL, 7.73 mmol) was then added via syringe. The mixture was heated at reflux for 16 h and then quenched by addition of H_2O, after cooling to room temperature. The product was extracted with CH_2Cl_2 (3 × 50 mL), and the combined organic extracts were washed with H_2O and then dried over Na_2SO_4. The crude product (yellow oil) was then purified by silica column chromatography (10% MeOH in CH_2Cl_2) to yield the pure product as a colorless oil. Yield: 0.880 g (46%). ^1H NMR (300 MHz, $CDCl_3$): δ 7.45 (s, 1H, imid), 7.05 (s, 1H, imid), 6.90 (s, 1H, imid), 5.77 (ddt, $^3J_{HH}$ = 16.9, 9.9, 6.6, 1H, C$\underline{H}$=CH_2), 4.90−5.07 (m, 2H, CH=C$\underline{H}_2$), 3.92 (t, $^3J_{HH}$ = 7.1, 2H, N-CH_2), 1.98−2.09 (m, 2H, CH_2), 1.78 (app. pent, J = 7, 2H, CH_2), 1.22−1.49 (m, 4H, CH_2). $^{13}C\{^1H\}$ NMR (75 MHz, $CDCl_3$): δ 138.5, 137.2, 129.5, 118.9, 114.9, 47.1, 33.6, 31.1, 28.4, 26.1. ESI-MS (CH_3CN, 180 °C, 3 kV): positive ion: 165.1391 m/z, $[M]H^+$ (calcd. 165.1386). Anal. Calcd for $C_{10}H_{16}N_2$ (164.25 g mol^{-1}): C, 73.13; H, 9.82; N, 17.06. Found: C, 72.97; H, 9.68; N, 16.96.

*$C\text{^}N\text{^}C\text{-}((CH_2)_5CH{=}CH_2)_2$ (**L2a**).* A mixture of 2,6-bis(bromomethyl)pyridine (1.30 g, 4.90 mmol) and 7-imidazole-1-heptene (2.41 g, 14.7 mmol) in 1,4-dioxane (50 mL) was heated at reflux for 5 h. The solvent was removed in vacuo to give an orange oil, which was then extracted with MeCN (50 mL). The filtrate was reduced in volume, and excess Et_2O was added to separate the product as an oil, which was separated by decantation. The remaining oil was washed with Et_2O (3 × 50 mL) before drying in vacuo to a yield a yellow foam. Yield: 2.737 g (94%). ^1H NMR (400 MHz, $CDCl_3$): δ 10.51 (b, 2H, imid), 8.17 (app. t, J = 2, 2H, imid), 7.73 (d, $^3J_{HH}$ = 7.6, 2H, py), 7.62 (dd, $^3J_{HH}$ = 8.3, 7.1, 1H, py), 7.37 (app. t, J = 2, 2H, imid), 5.73 (s, 4H, pyC$\underline{H}_2$), 5.65 (ddt, $^3J_{HH}$ = 16.9, 10.1, 6.7, 2H, C$\underline{H}$=CH_2), 4.88 (d app. q, $^3J_{HH}$ = 16.9, J = 2, 2H, CH=C$\underline{H}_2$), 4.83 (br d, $^3J_{HH}$ = 10.1, 2H, CH=C$\underline{H}_2$), 4.34 (t, $^3J_{HH}$ = 7.5, 4H, N-C$\underline{H}_2$$CH_2$), 1.94 (app. q, J = 7, 4H, CH_2), 1.86 (app. pent, J = 8, 4H, CH_2), 1.20−1.40 (m, 8H, CH_2). $^{13}C\{^1H\}$ NMR (101 MHz, $CDCl_3$): δ 153.3, 139.1, 138.2, 137.2, 137.1, 124.0, 123.9, 121.5, 115.0, 53.4, 50.1, 33.4, 30.3, 28.2, 25.6. ESI-MS (CH_3CN, 180 °C, 3 kV): positive ion: 216.6598 m/z, $[M]^{2+}$ (calcd. 216.6597). Anal. Calcd for $C_{27}H_{39}Br_2N_5$ (593.44 g mol^{-1}): C, 54.65; H, 6.62; N, 11.80. Found: C, 54.49; H, 6.57; N, 11.74.

*$[Rh(C\text{^}N\text{^}C\text{-}((CH_2)_5CH{=}CH_2)_2)(CO)][BAr^F{}_4]$ (**2a**).* A mixture of **L2a** (0.050 g, 0.084 mmol), Ag_2O (0.020 g, 0.084 mmol), and $Na[BAr^F{}_4]$ (0.075 g, 0.084 mmol) in CH_2Cl_2 (3 mL) was stirred in the absence of light for 16 h. A solution of $[Rh(CO)_2Cl]_2$ (0.016 g, 0.042 mmol) in CH_2Cl_2 (3 mL) was added, and the resulting suspension was stirred for a further 20 h. The suspension was filtered through a pad of silica, eluting with CH_2Cl_2, to yield the crude product upon removal of solvent. The crude material was then purified by precipitation from Et_2O−pentane to yield the pure product as a yellow powder. Yield: 0.070 g (58%). ^1H NMR (400 MHz, CD_2Cl_2): δ 7.86 (t, $^3J_{HH}$ = 7.7, 1H, py), 7.70−7.75 (m, 8H, Ar^F), 7.55 (br, 4H, Ar^F), 7.49 (d, $^3J_{HH}$ = 7.7, 2H, py), 7.14 (d, $^3J_{HH}$ = 1.9, 2H, imid), 6.99 (d, $^3J_{HH}$ = 2.0, 2H, imid), 5.75 (ddt, $^3J_{HH}$ = 16.9, 10.2, 6.7, 2H, C$\underline{H}$=CH_2), 5.46 (d, $^2J_{HH}$ = 14.7, 2H, pyC$\underline{H}_2$), 5.02 (d, $^2J_{HH}$ = 14.7, 2H, pyC$\underline{H}_2$), 4.94 (d app. q, $^3J_{HH}$ = 16.9, J = 2, 2H, CH=C$\underline{H}_2$), 4.89 (br d, $^3J_{HH}$ = 10.2, 2H, CH=C$\underline{H}_2$), 4.13 (t, $^3J_{HH}$ = 7.6, 4H, N-C$\underline{H}_2$$CH_2$), 2.02 (app. q, J = 7, 4H, CH_2), 1.82−1.95 (m, 4H, CH_2), 1.30−1.48 (m, 8H, CH_2). $^{13}C\{^1H\}$ NMR (101 MHz, CD_2Cl_2): δ 193.9 (d, $^1J_{RhC}$ = 79, carbonyl), 182.2 (d, $^1J_{RhC}$ = 41, carbene), 162.2 (q, $^1J_{CB}$ = 49, Ar^F), 156.0 (s, py), 141.4 (s, py), 139.1 (s, C$\underline{H}$=CH_2), 135.3 (s, Ar^F), 129.3 (q, $^2J_{CF}$ = 32, Ar^F), 125.1 (q, $^1J_{CF}$ = 272, Ar^F), 124.8 (s, py), 121.8 (s, imid), 121.3 (s, imid), 118.0 (sept, $^3J_{FC}$ = 4, Ar^F), 114.8 (s, CH=C$\underline{H}_2$), 55.8 (s,

dx.doi.org/10.1021/ic5024828 | Inorg. Chem. 2015, 54, 312−322

pyCH$_2$), 51.4 (s, N-CH$_2$CH$_2$), 34.0 (s, CH$_2$), 31.7 (s, CH$_2$), 28.8 (s, CH$_2$), 26.5 (s, CH$_2$). ESI-MS (CH$_3$CN, 180 °C, 3 kV): positive ion: 562.2067 *m/z*, [M]$^+$ (calcd. 562.2048). Anal. Calcd for $C_{60}H_{49}BF_{24}N_5ORh$ (1425.74 g mol^{-1}): C, 50.55; H, 3.46; N, 4.91. Found: C, 50.43; H, 3.36; N, 4.90. IR (CH$_2$Cl$_2$): ν(CO) 1978 cm^{-1}.

*[Rh(C^N^C-(CH$_2$)$_{12}$)(CO)][BAr$^F_4$] (**1a**).* Route 1: A mixture of **L1a** (0.100 g, 0.176 mmol), Ag$_2$O (0.041 g, 0.176 mmol), and Na[BAr$^F_4$] (0.170 g, 0.192 mmol) in CH$_2$Cl$_2$ (3 mL) was stirred in the absence of light for 16 h. A solution of [Rh(CO)$_2$Cl]$_2$ (0.034 g, 0.088 mmol) in CH$_2$Cl$_2$ (3 mL) was added, and the suspension was stirred for a further 5 h. The solution was filtered, and the filtrate was reduced to dryness to afford the crude product, which was then passed through a silica pad using CH$_2$Cl$_2$ as the eluent to give a vibrant yellow oil. The oil was then dissolved in Et$_2$O, and excess hexane was added to precipitate the product, which was isolated by filtration and washed with hexane to give **1a** as a yellow powder. Yield: 0.129 g (52%).

Route 2: N$_2$ was bubbled through a solution of **2a** (0.100 g, 0.070 mmol) and Grubbs I (0.003 g, 0.004 mmol) in CH$_2$Cl$_2$ (70 mL) for 1 h. After this time, ESI-MS indicated 69% reaction conversion. A further portion of Grubbs I (0.003 g, 0.004 mmol) was added, and N$_2$ was bubbled through for an additional hour, at which time ESI-MS indicated the reaction had gone to completion. The resulting solution was concentrated and passed through a silica pad using CH$_2$Cl$_2$ as the eluent to afford [Rh(C^N^C-C$_{12}$H$_{22}$)(CO)][BAr$^F_4$] as a yellow glass (cis:trans ∼ 1:3). Yield: 0.096 g (95%). A solution of [Rh(C^N^C-C$_{12}$H$_{22}$)(CO)][BAr$^F_4$] (0.096 g, 0.065 mmol) in CH$_2$Cl$_2$ (5 mL) was added to a J. Young's flask charged with palladium on carbon (10 wt % Pd, 0.014 g, 0.013 mmol, ca. 20 mol % Pd), and the solution was placed under H$_2$ (4 bar). After stirring for 72 h, the reaction mixture was degassed, concentrated, and filtered through a Celite pad. The filtrate was concentrated in vacuo to give **1a** as a yellow−orange foam. Yield: 0.075 g (82%).

Data for [Rh(C^N^C−C$_{12}$H$_{22}$)(CO)][BAr$^F_4$]: ^{1}H NMR (400 MHz, CD$_2$Cl$_2$, trans isomer only): δ 7.88 (t, $^3J_{HH}$ = 7.7, 1H, py), 7.70−7.75 (m, 8H, Ar^F), 7.55 (br, 4H, Ar^F), 7.50 (d, $^3J_{HH}$ = 7.7, 2H, py), 7.15 (d, $^3J_{HH}$ = 1.9, 2H, imid), 7.01 (d, $^3J_{HH}$ = 1.9, 2H, imid), 5.40 (br, 2H, pyCH$_2$), 5.35−5.39 (m, 2H,CH=CH), 5.03 (br, 2H, pyCH$_2$), 3.90−4.36 (m, 4H, N-CH$_2$CH$_2$), 1.14−2.24 (m, 16H, CH$_2$). ESI-MS (CH$_3$CN, 180 °C, 3 kV): positive ion: 534.1762 *m/z*, [M]$^+$ (calcd. 534.1735). Data for **1a**: ^{1}H NMR (500 MHz, CD$_2$Cl$_2$): δ 7.88 (t, $^3J_{HH}$ = 7.7, 1H, py), 7.70−7.75 (m, 8H, Ar^F), 7.56 (br, 4H, Ar^F), 7.51 (d, $^3J_{HH}$ = 7.7, 2H, py), 7.14 (d, $^3J_{HH}$ = 1.9, 2H, imid), 7.00 (d, $^3J_{HH}$ = 1.9, 2H, imid), 5.45 (d, $^2J_{HH}$ = 14.7, 2H, pyCH$_2$), 5.03 (d, $^2J_{HH}$ = 14.7, 2H, pyCH$_2$), 4.25−4.36 (m, 2H, *N*-CH$_2$CH2), 3.93−4.04 (m, 2H, N-CH$_2$), 1.77−2.01 (m, 4H, CH$_2$), 1.10−1.53 (m, 16H, CH$_2$). ^{13}C{^{1}H} NMR (101 MHz, CD$_2$Cl$_2$): δ 194.0 (d, $^1J_{RhC}$ = 80, carbonyl), 181.8 (d, $^1J_{RhC}$ = 42, carbene), 162.3 (q, $^1J_{BC}$ = 50, Ar^F), 156.0 (s, py), 141.5 (s, py), 135.4 (s, Ar^F), 129.4 (q, $^2J_{CF}$ = 32, Ar^F), 125.2 (q, $^1J_{CF}$ = 273, Ar^F), 124.9 (s, py), 121.9 (s, imid), 121.5 (s, imid), 118.0 (sept, $^3J_{FC}$ = 4, Ar^F), 55.9 (s, pyCH$_2$), 51.5 (s, N-CH$_2$CH$_2$), 31.6 (s, CH$_2$), 28.0 (s, CH$_2$), 27.9 (s, CH$_2$), 27.9 (s, CH$_2$), 24.6 (s, CH$_2$). ESI-MS (CH$_3$CN, 180 °C, 3 kV): positive ion: 536.1903 *m/z*, [M]$^+$ (calcd. 536.1891). Anal. Calcd for $C_{58}H_{47}BF_{24}N_5ORh$ (1399.70 g mol^{-1}): C, 49.77; H, 3.38; N, 5.00. Found: C, 49.92; H, 3.40; N, 5.21. IR (CH$_2$Cl$_2$): ν(CO) 1979 cm^{-1}. IR (C$_6$H$_6$): ν(CO) 1972 cm^{-1}.

*CNC-((CH$_2$)$_5$CH=CH$_2$)$_2$ (**L2b**).* A mixture of 2,6-bis(imidazolyl)-pyridine (0.634 g, 2.77 mmol) and 7-bromo-1-heptene (1.05 mL, 6.91 mmol) in 1,4-dioxane (2 mL) was stirred at 100 °C in a sealed Young's flask for 16 h. After cooling, the reaction mixture was extracted with MeCN (3 × 10 mL). To the filtrate was added Et$_2$O (20 mL) to form a white suspension, which was left to stand for 4 h before filtration. The remaining white solid was washed with Et$_2$O and dried in vacuo to give the product. Yield: 1.067 g (68%). ^{1}H NMR (300 MHz, CDCl$_3$): δ 11.92 (bs, 2H, imid), 9.27 (app. t, *J* = 2, 2H, imid), 8.78 (d, $^3J_{HH}$ = 8.2, 2H, py), 8.31 (t, $^3J_{HH}$ = 8.1, 1H, py), 7.52 (app. t, *J* = 2, 2H, imid), 5.75 (ddt, $^3J_{HH}$ = 16.9, 10.1, 6.7, 2H, CH=CH$_2$), 4.98 (d app. q, $^3J_{HH}$ = 16.9, *J* = 2, 2H, CH=CH$_2$), 4.93 (br d, $^3J_{HH}$ = 10.1, 2H, CH=CH$_2$), 4.59 (t, $^3J_{HH}$ = 7.3, 4H, N-CH$_2$), 1.95−2.12 (m, 8H, CH$_2$), 1.34−1.54 (m, 8H, CH$_2$). ^{13}C{^{1}H} NMR (75 MHz, CDCl$_3$): δ 145.4, 145.3, 138.3, 136.7, 123.3, 120.9, 115.6, 115.1, 50.9, 33.4, 30.3, 28.2, 25.7. ESI-MS (CH$_3$CN, 180 °C, 3 kV): positive ion: 202.6458 *m/z*, [M]$^{2+}$/2 (calcd. 202.6441). Anal. Calcd for $C_{25}H_{35}Br_2N_5$ (565.39 g mol^{-1}): C, 53.11; H, 6.24; N, 12.39. Found: C, 52.92; H, 6.11; N, 12.28.

*[Rh(CNC-((CH$_2$)$_5$CH=CH$_2$)$_2$)(CO)][BAr$^F_4$] (**2b**).* A mixture of **L2b** (0.100 g, 0.177 mmol), Ag$_2$O (0.041 g, 0.176 mmol), and Na[BAr$^F_4$] (0.173 g, 0.195 mmol) in CH$_2$Cl$_2$ (2 mL) was stirred in the absence of light for 16 h. The reaction mixture was filtered onto [Rh(CO)$_2$Cl]$_2$ (0.035 g, 0.088 mmol), and the resulting suspension was stirred for a further 5 min before further filtration. The filtrate was reduced to dryness and purified on silica (CH$_2$Cl$_2$) to afford the product as a purple foam on removal of the solvent. Yield: 0.218 g (83%). ^{1}H NMR (400 MHz, CD$_2$Cl$_2$): δ 8.01 (t, $^3J_{HH}$ = 8.2, 1H, py), 7.72−7.80 (m, 8H, Ar^F), 7.58 (br, 4H, Ar^F), 7.43 (d, $^3J_{HH}$ = 2.2, 2H, imid), 7.15 (d, $^3J_{HH}$ = 8.2, 2H, py), 7.10 (d, $^3J_{HH}$ = 2.2 Hz, 2H, imid), 5.81 (ddt, $^3J_{HH}$ = 16.9, 10.2, 6.7 Hz, 2H, CH=CH$_2$), 5.00 (d app. q, $^3J_{HH}$ = 16.9, *J* = 2, 2H, CH=CH$_2$), 4.95 (br d, $^3J_{HH}$ = 10.2, 2H, CH=CH$_2$), 4.14 (t, $^3J_{HH}$ = 7.5, 4H, *N*-CH$_2$), 2.08 (app. q, *J* = 7, 4H, CH$_2$), 1.93 (app. pent, *J* = 7, 4H, CH$_2$), 1.38−1.54 (m, 8H, CH$_2$). ^{13}C{^{1}H} NMR (101 MHz, CD$_2$Cl$_2$): δ 186.6 (d, $^1J_{RhC}$ = 48, carbene), 162.4 (q, $^1J_{CB}$ = 50, Ar^F), 152.7 (s, py), 146.3 (s, py), 139.0 (s, CH=CH$_2$), 135.4 (s, Ar^F), 129.5 (q, $^2J_{FC}$ = 32, Ar^F), 125.2 (q, $^1J_{FC}$ = 272, Ar^F), 123.8 (s, imid), 118.1 (sept, $^3J_{FC}$ = 4, Ar^F), 117.0 (s, imid), 115.0 (s, CH=CH$_2$), 106.7 (s, py), 53.0 (s, N-CH$_2$), 34.0 (s, CH$_2$), 31.6 (s, CH$_2$), 28.8 (s, CH$_2$), 26.4 (s, CH$_2$); carbonyl resonance not observed. ESI-MS (CH$_3$CN, 180 °C, 3 kV): positive ion: 534.1726 *m/z*, [M]$^+$ (calcd. 534.1735). Anal. Calcd for $C_{58}H_{45}BF_{24}N_5ORh$ (1397.69 g mol^{-1}): C, 49.84; H, 3.25; N, 5.01. Found: C, 49.72; H, 3.25; N, 5.12. IR (CH$_2$Cl$_2$): ν(CO) 1990 cm^{-1}. IR (CH$_3$CN): ν(CO) 1980 cm^{-1}.

*[Rh(CNC-(CH$_2$)$_{12}$)(CO)][BAr$^F_4$] (**1b**).* N$_2$ was bubbled through a solution of **2b** (0.100 g, 0.074 mmol) and Grubbs I (0.003 g, 0.004 mmol) in CH$_2$Cl$_2$ (70 mL) for 30 min (reaction completion observed by ESI-MS). The resulting solution was concentrated to dryness and purified on silica (CH$_2$Cl$_2$). [Rh(CNC-C$_{12}$H$_{22}$)(CO)][BAr$^F_4$] (cis:-trans ∼ 1:1) was obtained as a purple powder by precipitation from CH$_2$Cl$_2$ with excess pentane and subsequent filtration. Yield: 0.083 g (82%). A solution of [Rh(CNC-C$_{12}$H$_{22}$)(CO)][BAr$^F_4$] (0.050 g, 0.037 mol) and [Ir(COD)(py)(PCy$_3$)][BAr$^F_4$] (0.003 g, 0.004 mol) in CH$_2$Cl$_2$ (2 mL) was placed under hydrogen (1 bar). After stirring for 2 h, the reaction mixture was concentrated in vacuo. The residue was then purified on silica (CH$_2$Cl$_2$). The eluted solvent was concentrated to 2 mL before precipitation of the product with excess pentane. Complex **2b** as a dark green powder was obtained by filtration and washed with pentane (3 × 5 mL). Yield: 0.042 g (83%).

Data for [Rh(CNC-C$_{12}$H$_{22}$)(CO)][BAr$^F_4$]: ^{1}H NMR (400 MHz, CD$_2$Cl$_2$): δ 8.04 (t, $^3J_{HH}$ = 8.2, 1H, py), 7.70−7.75 (m, 8H, Ar^F), 7.56 (s, 4H, Ar^F), 7.48/7.49 (d, $^3J_{HH}$ = 2.3, 2H, imid), 7.17 (d, $^3J_{HH}$ = 8.1, 2H, py), 7.09/7.10 (d, $^3J_{HH}$ = 2.3, 2H, imid), 5.27−5.37 (m, 2H, CH=CH), 4.13−4.21 (m, 4H, N-CH$_2$), 1.97−2.09 (m, 4H, CH$_2$), 1.80−1.91 (m, 4H, CH$_2$), 1.24−1.50 (m, 8H, CH$_2$). ESI-MS (CH$_3$CN, 180 °C, 3 kV) positive ion: 506.1422 *m/z*, [M]$^+$ (calcd. 506.1422). Data for **1b**: ^{1}H NMR (500 MHz, CD$_2$Cl$_2$): δ 8.05 (t, $^3J_{HH}$ = 8.2, 1H, py), 7.70−7.75 (m, 8H, Ar^F), 7.56 (br, 4H, Ar^F), 7.49 (d, $^3J_{HH}$ = 2.3, 2H, imid), 7.18 (d, $^3J_{HH}$ = 8.2, 2H, py), 7.12 (d, $^3J_{HH}$ = 2.3, 2H, imid), 4.17 (t, $^3J_{HH}$ = 6.5, 4H, N-CH$_2$), 1.91 (app. p, *J* = 6, 4H, CH$_2$), 1.24−1.48 (m, 16H, CH$_2$). ^{13}C{^{1}H} NMR (101 MHz, CD$_2$Cl$_2$): δ 196.8 (d, $^1J_{RhC}$ = 78, carbonyl), 186.5 (d, $^1J_{RhC}$ = 48, carbene), 162.3 (q, $^1J_{CB}$ = 50, Ar^F), 152.7 (s, py), 146.3 (s, py), 135.4 (s, Ar^F), 129.5 (q, $^2J_{FC}$ = 32, Ar^F), 125.2 (q, $^1J_{FC}$ = 272, Ar^F), 123.2 (s, imid), 118.1 (sept, $^3J_{FC}$ = 4, Ar^F), 117.5 (s, imid), 106.7 (s, py), 51.7 (s, N-CH$_2$CH$_2$), 30.6 (s, CH$_2$), 29.0 (s, CH$_2$), 28.8 (s, CH$_2$), 28.5 (s, CH$_2$), 25.4 (s, CH$_2$). ESI-MS (CH$_3$CN, 180 °C, 3 kV): positive ion: 508.1570 *m/z*, [M]$^+$ (calcd. 508.1578). Anal. Calcd for $C_{56}H_{43}BF_{24}N_5ORh$ (1371.65 g mol^{-1}): C, 49.04; H, 3.16; N, 5.11. Found: C, 49.17; H, 3.07; N, 5.10. IR (CH$_2$Cl$_2$): ν(CO) 1986 cm^{-1}. IR (CH$_3$CN) ν(CO) 1977 cm^{-1}.

*[Rh(CNC-(CH$_2$)$_{12}$)(CO)(CH$_3$I)][BAr$^F_4$] (**3b**).* To a purple solution of **1b** (0.033 g, 0.024 mmol) in CH$_2$Cl$_2$ (5 mL) was added MeI (0.0075 mL, 0.120 mmol). The solution was stirred at room temperature for 3 h, and the product was precipitated by addition of excess pentane. The

dx.doi.org/10.1021/ic5024828 | *Inorg. Chem.* 2015, 54, 312−322

Table 2. Crystallographic Data

	1a	1a*	1b	3b	4b·$^1/_2CH_2Cl_2$	5·$^1/_3C_6H_6$
CCDC	1025594	1027503	1025595	1025596	1025597	1025598
formula	$C_{58}H_{47}BF_{24}N_5ORh$	$C_{58}H_{47}BF_{24}N_5ORh$	$C_{56}H_{43}BF_{24}N_5ORh$	$C_{57}H_{46}BF_{24}IN_5ORh$	$C_{56.5}H_{44}BCl_3F_{24}N_5ORh$	$C_{28}H_{36}N_5ORh$
M	1399.72	1399.72	1371.67	1513.61	1485.03	561.53
crystal system	triclinic	triclinic	monoclinic	monoclinic	triclinic	trigonal
space group	$P\bar{1}$	$P\bar{1}$	$P2_1/c$	$P2_1/c$	$P\bar{1}$	$R\bar{3}$
radiation	Mo Kα	Cu Kα	Mo Kα	Mo Kα	Mo Kα	Mo Kα
a [Å]	9.3661(3)	13.0450(10)	13.3809(5)	14.26866(15)	12.7330(4)	19.2242(2)
b [Å]	18.7809(6)	14.5880(14)	28.7207(11)	17.1057(2)	15.5875(4)	19.2242(2)
c [Å]	19.3860(6)	17.4059(11)	16.9649(7)	24.6768(3)	17.0556(5)	37.5121(8)
α [deg]	116.409(3)	104.723(7)	90	90	100.337(2)	90
β [deg]	94.878(3)	105.186(7)	105.369(4)	94.4576(10)	97.165(2)	90
γ [deg]	92.986(3)	102.973(8)	90	90	113.343(3)	120
V [Å^3]	3027.66(18)	2937.5(4)	6286.6(5)	6004.79(12)	2984.89(16)	12006.0(4)
Z	2	2	4	4	2	18
density [g cm^{-3}]	1.535	1.582	1.449	1.674	1.652	1.398
μ (mm^{-1})	0.400	3.452	0.384	0.918	0.541	0.669
θ range [deg]	$3.16 \le \theta \le 26.37$	$6.49 \le \theta \le 66.58$	$3.32 \le \theta \le 26.37$	$3.10 \le \theta \le 26.37$	$2.94 \le \theta \le 26.37$	$2.98 \le \theta \le 26.37$
reflns collected	23522	18880	96566	70014	29569	89168
R_{int}	0.0340	0.1078	0.0638	0.0348	0.0287	0.0444
completeness	99.8%	99.8%	99.8%	99.8%	99.8%	99.8%
no. of data/restr/param	12 359/852/960	10 378/830/924	12 828/1087/955	12 268/885/909	12 186/373/852	5442/459/389
R_1 [$I > 2\sigma(I)$]	0.0495	0.0803	0.0546	0.0446	0.0474	0.0374
wR_2 [all data]	0.1117	0.2151	0.1572	0.1141	0.1184	0.0958
GOF	1.051	1.018	1.040	1.053	1.037	1.078
largest diff. pk and hole [e Å^{-3}]	0.69/−0.53	0.89/−1.10	0.94/−0.59	2.62/−0.96	1.05/−0.92	1.75/−0.22

product as a cream powder was isolated by filtration, washed with pentane (2 × 5 mL), and dried in vacuo. Yield: 0.028 g (75%). ^{1}H NMR (500 MHz, CD_2Cl_2): δ 8.34 (t, $^3J_{HH}$ = 8.2, 1H, py), 7.78 (d, $^3J_{HH}$ = 2.2, 2H, imid), 7.70−7.74 (m, 8H, Ar^F), 7.56 (d, $^3J_{HH}$ = 8.2, 2H, py), 7.55 (br, 4H, Ar^F), 7.28 (d, $^3J_{HH}$ = 2.2, 2H, imid), 4.25 (app. t, J = 8, 4H, N-CH_2), 2.39−2.50 (m, 2H, N-$CH_2C\underline{H}_2$), 1.84−1.95 (m, 2H, N-$CH_2C\underline{H}_2$), 1.30−1.75 (m, 16H, CH_2), 0.59 (d, $^2J_{RhH}$ = 2.1, 3H, Rh-CH_3). ^{13}C{^{1}H} NMR (151 MHz, CD_2Cl_2): δ 189.8 (d, $^1J_{RhC}$ = 61, carbonyl), 180.2 ($^1J_{RhC}$ = 37, carbene), 162.3 (q, $^1J_{CB}$ = 50, Ar^F), 150.2 (s, py), 145.7 (s, py), 135.3 (s, Ar^F), 129.4 (q, $^2J_{CF}$ = 32, Ar^F), 125.1 (q, $^1J_{CF}$ = 272, Ar^F), 124.3 (s, imid), 118.2 (s, imid), 118.0 (sept, $^3J_{FC}$ = 4, Ar^F), 108.8 (s, py), 53.1 (s, N-CH_2), 30.1 (s, N-$CH_2C\underline{H}_2$), 29.5 (s, CH_2), 28.6 (s, CH_2), 28.5 (s, CH_2), 25.9 (s, CH_2), −2.1 (d, $^1J_{RhC}$ = 18, Rh-CH_3). ESI-MS (CH_3CN, 180 °C, 3 kV): positive ion: 650.0849 m/z, $[M]^+$ (calcd. 650.0858). Anal. Calcd for $C_{57}H_{46}BF_{24}IN_5ORh$ (1513.15 g mol^{-1}): C, 45.23; H, 3.06; N, 4.63. Found: C, 45.18; H, 2.97; N, 4.58. IR (CH_2Cl_2): ν(CO) 2070 cm^{-1}. IR (CH_3CN): ν(CO) 2066 cm^{-1}.

*[Rh(CNC-$(CH_2)_{12}$)(CO)Cl_2][BAr$^F{}_4$] (**4b**).* A solution of **1b** (0.020 g, 0.015 mmol) and $PhICl_2$ (0.004 g, 0.015 mmol) in CH_2Cl_2 (2 mL) was stirred at room temperature for 3 h. The reaction mixture was layered with pentane and left to stand for 16 h to give the yellow crystalline product, which was isolated by filtration washed with pentane (2 × 5 mL). Yield: 0.014 g (67%). ^{1}H NMR (500 MHz, CD_2Cl_2): δ 8.43 (t, $^3J_{HH}$ = 8.2, 1H, py), 7.84 (d, $^3J_{HH}$ = 2.2, 2H, imid), 7.70−7.75 (m, 8H, Ar^F), 7.64 (d, $^3J_{HH}$ = 8.2, 2H, py), 7.56 (s, 4H, Ar^F), 7.36 (d, $^3J_{HH}$ = 2.2, 2H, imid), 4.41 (t, $^3J_{HH}$ = 7.7, 4H, N-CH_2), 2.09 (app. p, J = 7, 4H, N-$CH_2C\underline{H}_2$), 1.56 (app. p, J = 6, 4H, CH_2), 1.34−1.51 (m, 12H, CH_2). ^{13}C{^{1}H} NMR (101 MHz, CD_2Cl_2): δ 181.6 (d, $^1J_{RhC}$ = 57, carbonyl), 173.9 (d, $^1J_{RhC}$ = 33, carbene), 162.3 (q, $^1J_{CB}$ = 49, Ar^F), 150.9 (s, py), 147.6 (s, py), 135.4 (s, Ar^F), 129.5 (q, $^2J_{CF}$ = 32, Ar^F), 125.2 (q, $^1J_{FC}$ = 272, Ar^F), 124.7 (s, imid), 119.1 (s, imid), 118.1 (sept, $^3J_{FC}$ = 4, Ar^F), 109.9 (s, py), 53.3 (s, N-CH_2), 31.1 (s, N-$CH_2C\underline{H}_2$), 29.2 (s, CH_2), 28.6 (s, CH_2), 28.1 (s, CH_2), 25.6 (s, CH_2). ESI-MS (CH_3CN, 180 °C, 3 kV): positive ion: 578.0958 m/z, $[M]^+$ (calcd. 578.0955). Anal. Calcd for $C_{56}H_{43}BCl_2F_{24}N_5ORh$ (1442.57 g mol^{-1}): C, 46.63; H, 3.00; N, 4.85. Found: C, 46.52; H, 2.85; N, 4.89. IR (CH_2Cl_2): ν(CO) 2111 cm^{-1}.

[Rh(C^N^C-$(CH_2)_{12}$)(CO)] (**5**).* To a J. Young's NMR tube charged with **1a** (0.020 g, 0.014 mmol) and K[$N(SiMe_3)_2$] (0.004 g, 0.020 mmol) was added C_6D_6 (0.5 mL) under an argon atmosphere. This resulted in the formation of a red solution and brown precipitate. Quantitative formation of **5** was observed by ^{1}H NMR spectroscopy alongside $HN(SiMe_3)_2$ (δ_{CH3} = 0.10, δ_{NH} = −0.07). The red solution was separated by decantation and layered with pentane (under argon). Diffusion of the solvent over 4 h afforded dark red crystals, which were isolated by decantation, washed with pentane, and dried. Yield: 0.003 g (52%). The extremely high reactivity of **5** has prevented accurate elemental analysis results from being obtained (on two separate sample batches). Complex **5** is best characterized directly in situ by NMR spectroscopy (see Figures S25−27 for ^{1}H and ^{13}C{^{1}H} NMR spectra). ^{1}H NMR (500 MHz, C_6D_6, 280 K): δ 6.61 (app. t, J = 1, 1H, imid), 6.37 (ddd, $^3J_{HH}$ = 9.1, 5.9, J = 1, 1H, py), 6.30 (app. t, J = 1, 1H, imid), 6.23 (d app. t, $^3J_{HH}$ = 9.1, J = 1, 1H, py), 6.15 (app. t, J = 1, 1H, imid), 5.99 (app. t, J = 1, 1H, imid), 5.81 (bd, J = 1, 1H, pyC$\underline{H}$), 5.36 (d app. t, $^3J_{HH}$ = 5.8, J = 1, 1H, py), 4.60 (app. t, J = 13, 1H, N-C$\underline{H}_2CH_2$), 4.58 (d, $^2J_{HH}$ = 13, 1H, pyC$\underline{H}_2$), 4.25 (app. t, J = 13, 1H, N-C$\underline{H}_2CH_2$), 3.72 (d, $^2J_{HH}$ = 12.8, 1H, pyC$\underline{H}_2$), 3.32−3.40 (m, 1H, N-C$\underline{H}_2CH_2$), 3.08−3.22 (m, 1H, N-C$\underline{H}_2CH_2$), 1.94−2.07 (m, 1H, CH_2), 1.72−1.83 (m, 1H, CH_2), 1.03−1.63 (m, 18H, CH_2). ^{1}H NMR (500 MHz, C_6D_6): δ 6.63 (app. t, J = 1, 1H, imid), 6.35 (dd, $^3J_{HH}$ = 9.1, 5.9, 1H, py), 6.33 (app. t, J = 1, 1H, imid), 6.20 (d, $^3J_{HH}$ = 9.0, 1H, py), 6.19 (app. t, J = 2, 1H, imid), 6.04 (app. t, J = 1, 1H, imid), 5.79 (br, 1H, pyC$\underline{H}$), 5.35 (d, $^3J_{HH}$ = 5.8, 1H, py), 4.58 (app. br, 2H, pyC$\underline{H}_2$ + N-C$\underline{H}_2CH_2$), 4.23 (s, 1H, N-C$\underline{H}_2CH_2$), 3.76 (bs, 1H, pyC$\underline{H}_2$), 3.41 (br, 1H, N-C$\underline{H}_2CH_2$), 3.22 (br, 1H, N-C$\underline{H}_2CH_2$), 1.99 (br, 1H, CH_2), 1.75 (br, 1H, CH_2), 1.00−1.66 (m, 18H, CH_2). ^{13}C{^{1}H} NMR (101 MHz, C_6D_6): δ 197.4 (d, $^1J_{RhC}$ = 73, carbonyl) 185.5 (d, $^1J_{RhC}$ = 43, carbene), 174.2 (d, $^1J_{RhC}$ = 44, carbene), 149.5 (s, py), 143.2 (s, py), 126.6 (s, py), 119.7 (s, py), 119.5 (s, imid), 119.3 (s, imid), 119.1 (s, imid), 117.7 (s, imid), 100.1 (s, py), 94.4 (s, py$\underline{C}$H), 58.2 (s, py$\underline{C}H_2$), 51.4 (s, N-$\underline{C}H_2CH_2$), 50.7 (s, N-$\underline{C}H_2CH_2$), 32.1 (s, CH_2), 31.0 (s,

dx.doi.org/10.1021/ic5024828 | Inorg. Chem. 2015, 54, 312−322

CH_2), 28.0 (s, CH_2), 27.8 (s, CH_2), 27.7 (s, CH_2), 27.6 (s, CH_2), 26.5 (s, CH_2), 24.8 (s, CH_2), 24.0 (s, CH_2). IR (C_6H_6): ν(CO): 1929 cm^{-1}.

In Situ NMR Experiments. *Preparation of [Rh(C^N^C-$(CH_2)_{12}$)(CO)(CH_3)I][BAr^F_4] (**3a**).* To a solution of **1a** (0.008 g, 0.006 mmol) in CD_2Cl_2 (0.5 mL) inside a J. Young's NMR tube was added MeI (0.018 mL, 0.285 mmol) under an argon atmosphere. The J. Young's NMR tube was sealed and monitored periodically by ^1H NMR spectroscopy. After 3 h, less than 5% **1a** was present. The reaction tube was left to stand for a further 17 h, after which no signals of **1a** were observable. The product **3a** was characterized in situ by NMR spectroscopy. ESI-MS and IR data were obtained from crude (impure) mixtures of **3a** prepared in a similar manner, with excess MeI removed in vacuo. ^1H NMR (500 MHz, CD_2Cl_2): δ 8.04 (t, $^3J_{HH}$ = 7.8, 1H, py), 7.70−7.75 (m, 8H, Ar^F), 7.63 (d, $^3J_{HH}$ = 7.8, 2H, py), 7.55 (br, 4H, Ar^F), 7.26 (d, $^3J_{HH}$ = 1.7, 2H, imid), 7.19 (d, $^3J_{HH}$ = 1.7, 2H, imid), 5.4 (br, 2H, pyCH_2), 5.1 (vbr, 2H, N-C$H_2$$CH_2$), 4.1 (br, 2H, N-C$H_2$$CH_2$), 1.76−2.05 (br m, 4H, CH_2), 1.23−1.55 (m, CH_2, 16H), 1.20 (d, $^2J_{RhH}$ = 1.8, Rh-Me); one pyCH_2 resonance (2H) was too broad to definitively locate at this temperature. $^{13}C\{^1H\}$ NMR (126 MHz, CD_2Cl_2, selected data only): δ 189.4 (d, $^1J_{RhC}$ = 64, carbonyl), 165.1 (d, $^1J_{RhC}$ = 34, carbene), −1.2 (d, $^2J_{RhH}$ = 20, Rh-CH_3). ESI-MS (CH_3CN, 180 °C, 3 kV) positive ion: 678.1169 m/z, $[M]^+$ (calcd. 678.1171). IR (CH_2Cl_2): ν(CO) 2067 cm^{-1}.

*Preparation of [Rh(C^N^C-$(CH_2)_{12}$)(CO)Cl_2][BAr^F_4] (**4a**).* To a J. Young's NMR tube charged with **1a** (0.008 g, 0.006 mmol) and $PhICl_2$ (0.002 g, 0.007 mmol) was added CD_2Cl_2 (0.5 mL) under an argon atmosphere. This resulted in a rapid color change from yellow to pale yellow and quantitative formation of **4a**, which was characterized immediately in situ by NMR spectroscopy. ESI-MS and IR data were obtained from crude (impure) mixtures of **4a** prepared in a similar manner and passed through a silica plug. ^1H NMR (500 MHz, CD_2Cl_2): δ 8.09 (t, $^3J_{HH}$ = 7.7, 1H, py), 7.70−7.75 (m, 8H, Ar^F), 7.68 (d, $^3J_{HH}$ = 7.8, 2H, py), 7.56 (br, 4H, Ar^F), 7.34 (d, $^3J_{HH}$ = 1.6, 2H, imid), 7.26 (d, $^3J_{HH}$ = 1.8, 2H, imid), 6.63 (d, $^2J_{HH}$ = 15.8, 2H, pyCH_2), 5.21 (d, $^2J_{HH}$ = 15.8, 2H, pyCH_2), 4.65 (ddd, $^2J_{HH}$ = 14.7, $^3J_{HH}$ = 12.8, 4.2, 2H, N-CH_2), 4.12 (ddd, $^2J_{HH}$ = 14.7, $^3J_{HH}$ = 12.5, 5.7, 2H, N-C$H_2$$CH_2$), 1.98−2.11 (m, 2H, CH_2), 1.86−1.98 (m, 2H, CH_2), 1.38−1.61 (m, 10H, CH_2), 1.12−1.36 (m, 6H, CH_2). $^{13}C\{^1H\}$ NMR (126 MHz, CD_2Cl_2, selected data only): δ 180.7 (d, $^1J_{RhC}$ = 57, carbonyl), 160.1 (d, $^1J_{RhC}$ = 30, carbene). ESI-MS (CH_3CN, 180 °C, 3 kV) positive ion: 606.1271 m/z, $[M]^+$ (calcd. 606.1268). IR (CH_2Cl_2): ν(CO) 2110 cm^{-1}.

X-ray Crystallography. Crystallographic data for **1a**, **1a***, **1b**, **3b**, **4b**, and **5** are summarized in Table 2. Data were collected on an Oxford Diffraction Gemini Ruby CCD diffractometer using graphite monochromated Mo Kα (λ = 0.71073 Å) or Cu Kα (λ = 1.54178 Å) radiation and a low-temperature device [150(2) K]. Data were collected and reduced using CrysAlisPro.[38] All non-hydrogen atoms were refined anisotropically using SHELXL,[39] through the Olex2 interface.[40] Hydrogen atoms were placed in calculated positions using the riding model. Full crystallographic details are documented in CIF format and have been deposited with the Cambridge Crystallographic Data Centre (see Table 2). These data can be obtained free of charge via www.ccdc.cam.ac.uk/data_request/cif.

■ ASSOCIATED CONTENT

Supporting Information

X-ray crystallographic data for complexes **1a**, **1a***, **1b**, **3b**, **4b**, and **5** in CIF format. Selected NMR and UV−vis absorption spectra. This material is available free of charge via the Internet at http://pubs.acs.org.

■ AUTHOR INFORMATION

Corresponding Author

*E-mail: a.b.chaplin@warwick.ac.uk.

Notes

The authors declare no competing financial interest.

■ ACKNOWLEDGMENTS

We thank the University of Warwick (R.E.A.) and the Royal Society (A.B.C.) for financial support. Crystallographic data was collected using a diffractometer purchased through support from Advantage West Midlands and the European Regional Development Fund.

■ REFERENCES

(1) (a) *Organometallic Pincer Chemistry*; van Koten, G., Milstein, D., Eds.; Springer: New York, 2013; Vol. *40*, pp 1−352. (b) Albrecht, M.; Lindner, M. M. *Dalton Trans.* **2011**, *40*, 8733−8744. (c) van der Boom, M. E.; Milstein, D. *Chem. Rev.* **2003**, *103*, 1759−1792. (d) Albrecht, M.; van Koten, G. *Angew. Chem., Int. Ed.* **2001**, *40*, 3750−3781.

(2) (a) Yao, W.; Zhang, Y.; Jia, X.; Huang, Z. *Angew. Chem., Int. Ed.* **2014**, *53*, 1390−1394. (b) Haibach, M. C.; Kundu, S.; Brookhart, M.; Goldman, A. S. *Acc. Chem. Res.* **2012**, *45*, 947−958. (c) Choi, J.; MacArthur, A. H. R.; Brookhart, M.; Goldman, A. S. *Chem. Rev.* **2011**, *111*, 1761−1779.

(3) (a) Feller, M.; Diskin-Posner, Y.; Shimon, L. J. W.; Ben-Ari, E.; Milstein, D. *Organometallics* **2012**, *31*, 4083−4101. (b) Schwartsburd, L.; Iron, M. A.; Konstantinovski, L.; Ben-Ari, E.; Milstein, D. *Organometallics* **2011**, *30*, 2721−2729.

(4) Selected examples: (a) Chang, Y.-H.; Nakajima, Y.; Tanaka, H.; Yoshizawa, K.; Ozawa, F. *J. Am. Chem. Soc.* **2013**, *135*, 11791−11794. (b) Filonenko, G. A.; Conley, M. P.; Copéret, C.; Lutz, M.; Hensen, E. J. M.; Pidko, E. A. *ACS Catal.* **2013**, *3*, 2522−2526. (c) van der Vlugt, J. I.; Pidko, E. A.; Bauer, R. C.; Gloaguen, Y.; Rong, M. K.; Lutz, M. *Chem.—Eur. J.* **2011**, *17*, 3850−3854. (d) Gunanathan, C.; Milstein, D. *Acc. Chem. Res.* **2011**, *44*, 588−602. (e) Balaraman, E.; Gnanaprakasam, B.; Shimon, L. J. W.; Milstein, D. *J. Am. Chem. Soc.* **2010**, *132*, 16756−16758. (f) van der Vlugt, J. I.; Siegler, M. A.; Janssen, M.; Vogt, D.; Spek, A. L. *Organometallics* **2009**, *28*, 7025−7032. (g) van der Vlugt, J. I.; Reek, J. N. H. *Angew. Chem., Int. Ed.* **2009**, *48*, 8832−8846. (h) Kohl, S. W.; Weiner, L.; Schwartsburd, L.; Konstantinovski, L.; Shimon, L. J. W.; Ben-David, Y.; Iron, M. A.; Milstein, D. *Science* **2009**, *324*, 74−77. (i) Tanaka, R.; Yamashita, M.; Nozaki, K. *J. Am. Chem. Soc.* **2009**, *131*, 14168−14169. (j) Gunanathan, C.; Ben-David, Y.; Milstein, D. *Science* **2007**, *317*, 790−792.

(5) (a) Filonenko, G. A.; Cosimi, E.; Lefort, L.; Conley, M. P.; Copéret, C.; Lutz, M.; Hensen, E. J. M.; Pidko, E. A. *ACS Catal.* **2014**, *4*, 2667−2671. (b) Hernández-Juárez, M.; Vaquero, M.; Álvarez, E.; Salazar, V.; Suárez, A. *Dalton Trans.* **2013**, *42*, 351−354. (c) Sun, Y.; Koehler, C.; Tan, R.; Annibale, V. T.; Song, D. *Chem. Commun.* **2011**, *47*, 8349−8351.

(6) Reviews: (a) Poyatos, M.; Mata, J. A.; Peris, E. *Chem. Rev.* **2009**, *109*, 3677−3707. (b) Pugh, D.; Danopoulos, A. A. *Coord. Chem. Rev.* **2007**, *251*, 610−641. (c) Peris, E.; Crabtree, R. H. *Coord. Chem. Rev.* **2004**, *248*, 2239−2246. Other selected examples: (d) Serra, D.; Cao, P.; Cabrera, J.; Padilla, R.; Rominger, F.; Limbach, M. *Organometallics* **2011**, *30*, 1885−1895. (e) Schultz, K. M.; Goldberg, K. I.; Gusev, D. G.; Heinekey, D. M. *Organometallics* **2011**, *30*, 1429−1437. (f) Inamoto, K.; Kuroda, J.-I.; Kwon, E.; Hiroya, K.; Doi, T. *J. Organomet. Chem.* **2009**, *694*, 389−396. (g) Wei, W.; Qin, Y.; Luo, M.; Xia, P.; Wong, M. S. *Organometallics* **2008**, *27*, 2268−2272. (h) Danopoulos, A. A.; Pugh, D.; Wright, J. A. *Angew. Chem., Int. Ed.* **2008**, *47*, 9765−9767. (i) Danopoulos, A. A.; Wright, J. A.; Motherwell, W. B.; Ellwood, S. *Organometallics* **2004**, *23*, 4807−4810. (j) Douthwaite, R. E.; Houghton, J.; Kariuki, B. M. *Chem. Commun.* **2004**, 698−699.

(7) Representative examples: (a) Hahn, F. E.; Jahnke, M. C.; Pape, T. *Organometallics* **2007**, *26*, 150−154. (b) Hahn, F. E.; Jahnke, M. C.; Gomez-Benitez, V.; Morales-Morales, D.; Pape, T. *Organometallics* **2005**, *24*, 6458−6463. (c) Nielsen, D. J.; Cavell, K. J.; Skelton, B. W.; White, A. H. *Inorg. Chim. Acta* **2002**, *327*, 116−125. (d) Gründemann, S.; Albrecht, M.; Loch, J. A.; Faller, J. W.; Crabtree, R. H. *Organometallics* **2001**, *20*, 5485−5488. (e) Peris, E.; Mata, J.; Loch, J. A.; Crabtree, R. H. *Chem. Commun.* **2001**, 201−202.

(8) (a) Chianese, A. R.; Drance, M. J.; Jensen, K. H.; McCollom, S. P.; Yusufova, N.; Shaner, S. E.; Shopov, D. Y.; Tendler, J. A. *Organometallics* **2014**, *33*, 457−464. (b) Chianese, A. R.; Shaner, S. E.; Tendler, J. A.; Pudalov, D. M.; Shopov, D. Y.; Kim, D.; Rogers, S. L.; Mo, A. *Organometallics* **2012**, *31*, 7359−7367. (c) Chianese, A. R.; Mo, A.; Lampland, N. L.; Swartz, R. L.; Bremer, P. T. *Organometallics* **2010**, *29*, 3019−3026.
(9) (a) Meyer, K.; Dalebrook, A. F.; Wright, L. J. *Dalton Trans.* **2012**, *41*, 14059−14067. (b) Saito, S.; Azumaya, I.; Watarai, N.; Kawasaki, H.; Yamasaki, R. *Heterocycles* **2009**, *79*, 531−548.
(10) Crowley, J. D.; Goldup, S. M.; Lee, A.-L.; Leigh, D. A.; McBurney, R. T. *Chem. Soc. Rev.* **2009**, *38*, 1530.
(11) Andrew, R. E.; Chaplin, A. B. *Dalton Trans.* **2014**, *43*, 1413−1423.
(12) (a) Frey, G. D.; Rentzsch, C. F.; von Preysing, D.; Scherg, T.; Mühlhofer, M.; Herdtweck, E.; Herrmann, W. A. *J. Organomet. Chem.* **2006**, *691*, 5725−5738. (b) Poyatos, M.; Uriz, P.; Mata, J. A.; Claver, C.; Fernandez, E.; Peris, E. *Organometallics* **2003**, *22*, 440−444.
(13) Wilson, J. M.; Sunley, G. J.; Adams, H.; Haynes, A. *J. Organomet. Chem.* **2005**, *690*, 6089−6095.
(14) Wright, J. A.; Danopoulos, A. A.; Motherwell, W. B.; Carroll, R. J.; Ellwood, S.; Saßmannshausen, J. *Chem. Ber.* **2006**, *2006*, 4857−4865.
(15) Simons, R. S.; Custer, P.; Tessier, C. A.; Youngs, W. J. *Organometallics* **2003**, *22*, 1979−1982.
(16) (a) Wucher, B.; Moser, M.; Schumacher, S. A.; Rominger, F.; Kunz, D. *Angew. Chem., Int. Ed.* **2009**, *48*, 4417−4421. (b) Moser, M.; Wucher, B.; Kunz, D.; Rominger, F. *Organometallics* **2007**, *26*, 1024−1030.
(17) For examples, see: (a) Nielsen, D. J.; Cavell, K. J.; Skelton, B. W.; White, A. H. *Inorg. Chim. Acta* **2006**, *359*, 1855−1869. (b) Loch, J. A.; Albrecht, M.; Peris, E.; Mata, J.; Faller, J. W.; Crabtree, R. H. *Organometallics* **2002**, *21*, 700−706.
(18) For examples, see: (a) Nawara-Hultzsch, A. J.; Stollenz, M.; Barbasiewicz, M.; Szafert, S.; Lis, T.; Hampel, F.; Bhuvanesh, N.; Gladysz, J. A. *Chem.—Eur. J.* **2014**, *20*, 4617−4637. (b) Zeits, P. D.; Rachiero, G. P.; Hampel, F.; Reibenspies, J. H.; Gladysz, J. A. *Organometallics* **2012**, *31*, 2854−2877. (c) Ayme, J.-F.; Lux, J.; Sauvage, J.-P.; Sour, A. *Chem.—Eur. J.* **2012**, *18*, 5565−5573. (d) Goldup, S. M.; Leigh, D. A.; Lusby, P. J.; McBurney, R. T.; Slawin, A. M. Z. *Angew. Chem., Int. Ed.* **2008**, *47*, 6999−7003. (e) Nawara, A.; Shima, T.; Hampel, F.; Gladysz, J. *J. Am. Chem. Soc.* **2006**, *128*, 4962−4963. (f) Fuller, A.-M. L.; Leigh, D. A.; Lusby, P. J.; Slawin, A. M. Z.; Walker, D. B. *J. Am. Chem. Soc.* **2005**, *127*, 12612−12619. (g) Chambron, J.-C.; Collin, J.-P.; Heitz, V.; Jouvenot, D.; Kern, J.-M.; Mobian, P.; Pomeranc, D.; Sauvage, J.-P. *Eur. J. Org. Chem.* **2004**, *2004*, 1627−1638.
(19) (a) Wang, L.; Hampel, F.; Gladysz, J. A. *Angew. Chem., Int. Ed.* **2006**, *45*, 4372−4375. (b) Wang, L.; Shima, T.; Hampel, F.; Gladysz, J. *Chem. Commun.* **2006**, *2006*, 4075−4077. (c) Bauer, E. B.; Ruwwe, J.; Hampel, F. A.; Szafert, S.; Gladysz, J. A.; Martín-Alvarez, J. M.; Peters, T. B.; Bohling, J. C.; Lis, T. *Chem. Commun.* **2000**, 2261−2262.
(20) Raba, A.; Anneser, M. R.; Jantke, D.; Cokoja, M.; Herrmann, W. A.; Kühn, F. E. *Tetrahedron Lett.* **2013**, *54*, 3384−3387.
(21) No reaction is observed when placing pure **1b** under H_2 (4 atm), implicating the external hydrogenation catalyst in this decomposition/undesired reactivity.
(22) Vazquez-Serrano, L. D.; Owens, B. T.; Buriak, J. M. *Inorg. Chim. Acta* **2006**, *359*, 2786−2797.
(23) Miecznikowski, J. R.; Gründemann, S.; Albrecht, M.; Mégret, C.; Clot, E.; Faller, J. W.; Eisenstein, O.; Crabtree, R. H. *Dalton Trans.* **2003**, 831−838.
(24) We are currently investigating the reaction of **1a** with carbon monoxide. Full details will be reported in due course; however, we do note here that placing **1a** under a carbon monoxide atmosphere induces atropisomerization, consistent with coordination of carbon monoxide. Similar dynamics has been studied in related palladium NHC systems, which are promoted by coordination of the counter anion.[23] The solution of the symmetrical polymorph **1a** contains a highly disordered solvent molecule that was removed using the SQUEEZE algorithm Spek, A. L. *Acta Crystallogr.* **2009**, *D65*, 148−155 whereas no solvent is present in the solution of **1a***, alternatively implicating crystal-packing effects..
(25) Feller, M.; Ben-Ari, E.; Gupta, T.; Shimon, L. J. W.; Leitus, G.; Diskin-Posner, Y.; Weiner, L.; Milstein, D. *Inorg. Chem.* **2007**, *46*, 10479−10490.
(26) (a) Bera, J. K.; Dunbar, K. R. *Angew. Chem., Int. Ed.* **2002**, *41*, 4453−4457. (b) Connick, W. B.; Marsh, R. E.; Schaefer, W. P.; Gray, H. B. *Inorg. Chem.* **1997**, *36*, 913−922. (c) Novoa, J. J.; Aullón, G.; Alemany, P.; Alvarez, S. *J. Am. Chem. Soc.* **1995**, *117*, 7169−7171. (d) *Extended Linear Chain Compounds*; Miller, J. S, Ed.; Plenum Press: New York, 1982; Vol. 3. (e) Mann, K. R.; Gordon, J. G.; Gray, H. B. *J. Am. Chem. Soc.* **1975**, *97*, 3553−3555. (f) Krogmann, K. *Angew. Chem., Int. Ed.* **1969**, *8*, 35−42.
(27) Selected rhodium examples: (a) Laurila, E.; Oresmaa, L.; Hassinen, J.; Hirva, P.; Haukka, M. *Dalton Trans.* **2013**, *42*, 395−398. (b) Inoki, D.; Matsumoto, T.; Nakai, H.; Ogo, S. *Organometallics* **2012**, *31*, 2996−3001. (c) Mitsumi, M.; Umebayashi, S.; Ozawa, Y.; Tadokoro, M.; Kawamura, H.; Toriumi, K. *Chem. Lett.* **2004**, *33*, 970−971. (d) Prater, M. E.; Pence, L. E.; Clérac, R.; Finniss, G. M.; Campana, C.; Auban-Senzier, P.; Jérome, D.; Canadell, E.; Dunbar, K. R. *J. Am. Chem. Soc.* **1999**, *121*, 8005−8016.
(28) (a) Helps, I. M.; Matthes, K. E.; Parker, D.; Ferguson, G. *J. Chem. Soc., Dalton Trans.* **1989**, 915−920. (b) Ferguson, G.; Matthes, K. E.; Parker, D. *J. Chem. Soc., Chem. Commun.* **1987**, 1350−1351.
(29) (a) Tran, N. T.; Stork, J. R.; Pham, D.; Olmstead, M. M.; Fettinger, J. C.; Balch, A. L. *Chem. Commun.* **2006**, 1130. (b) Mann, K. R.; Thich, J. A.; Bell, R. A.; Coyle, C. L.; Gray, H. B. *Inorg. Chem.* **1980**, *19*, 2462−2468. (c) Mann, K. R.; Lewis, N. S.; Williams, R. M.; Gray, H. B.; Gordon, J. G. *Inorg. Chem.* **1978**, *17*, 828−834.
(30) Rice, S. F.; Gray, H. B. *J. Am. Chem. Soc.* **1981**, *103*, 1593−1595.
(31) Hartwig, J. F. *Organotransition Metal Chemistry*; University Science Books: Sausalito, CA, 2010.
(32) Taylor, R. T.; Stevenson, T. A. *Tetrahedron Lett.* **1988**, *29*, 2033−2036.
(33) Feller, M.; Diskin-Posner, Y.; Leitus, G.; Shimon, L. J. W.; Milstein, D. *J. Am. Chem. Soc.* **2013**, *135*, 11040−11047.
(34) Schaub, T.; Radius, U.; Diskin-Posner, Y.; Leitus, G.; Shimon, L. J. W.; Milstein, D. *Organometallics* **2008**, *27*, 1892−1901.
(35) (a) Gloaguen, Y.; Rebreyend, C.; Lutz, M.; Kumar, P.; Huber, M.; van der Vlugt, J. I.; Schneider, S.; de Bruin, B. *Angew. Chem., Int. Ed.* **2014**, *53*, 6814−6818. (b) Khaskin, E.; Diskin-Posner, Y.; Weiner, L.; Leitus, G.; Milstein, D. *Chem. Commun.* **2013**, *49*, 2771−2773. (c) Schwartsburd, L.; Iron, M. A.; Konstantinovski, L.; Diskin-Posner, Y.; Leitus, G.; Shimon, L. J. W.; Milstein, D. *Organometallics* **2010**, *29*, 3817−3827. (d) Ben-Ari, E.; Leitus, G.; Shimon, L. J. W.; Milstein, D. *J. Am. Chem. Soc.* **2006**, *128*, 15390−15391.
(36) Buschmann, W. E.; Miller, J. S.; Bowman-James, K.; Miller, C. N. *Inorg. Synth.* **2002**, *33*, 83−91.
(37) McCleverty, J. A.; Wilkinson, G.; Lipson, L. G.; Maddox, M. L.; Kaesz, H. D. *Inorg. Synth.* **1990**, *28*, 84−86.
(38) *CrysAlisPro*; Oxford Diffraction Ltd: Abingdon, England, 2014.
(39) Sheldrick, G. M. *Acta Crystallogr.* **2008**, *A64*, 112−122.
(40) Dolomanov, O. V.; Bourhis, L. J.; Gildea, R. J.; Howard, J. A. K.; Puschmann, H. *J. Appl. Crystallogr.* **2009**, *42*, 339−341.